An Investigation of the SHIV reservoirs in the lymphoid organs of HIV-vaccinated rhesus monkeys after SHIV challenge.

Kealan Timothy Benn

This Dissertation is submitted in fulfilment of the requirements for the degree of Master of Science in the Department of Pathology, Division of Medical Virology, University of Cape Town.

2021

Table of Contents

Contents

PLAGIARISM DECLARATION 4

DECLARATION 5

ACKNOWLEDGEMENTS 6

ABBREVIATIONS: 7

List of Figures 10

List of Tables: 11

ABSTRACT 12

Literature Review 14

1.1 State of HIV/AIDS epidemic 14

1.2 Structure and properties of HIV 16

1.3 HIV Replication 19

1.4 SHIV 24

Simian-human immunodeficiency viruses 24

1.5 HIV Immune Responses 25

1.6 The HIV-1 envelope protein and its role in immune evasion 26

1.7 Reservoir Formation 26

1.8 Nonhuman primate models to test HIV vaccine candidates. 30

1.9 Project Rationale 32

1.10 Aims. 33

Materials and Methods 34

2.1 Background information of samples used in the study. 34

2.1.1 Biological samples used in this study. 34

2.1.2 Information on experimental animals from which samples were derived. 35

2.1.3 Preparation of samples and acknowledgements 36

2.2 DNA and RNA Extraction from PBMCs and splenocytes and lymphoid cells. 36

2.3 Measurement of RNA and DNA levels in tissues 39

2.3.1 RNA viral load assay 40

2.3.2 Proviral DNA Assay 41

2.4 Preparation of cell lysates from cells infected with modified vaccinia Ankara (MVA) expressing HIV-1 Env and SIV Gag for Western blotting. 44

2.4.1 Infection and subsequent harvesting of lysates from HEK293T cells infected with MVA expressing HIV-1 Env and SIV Gag 44

2.5 HIV envelope ELISA 47

2.6 Single Genome Amplification (SGA) 49
2.6.1 cDNA synthesis 49
2.6.2 Amplification & sequencing 50
Results 53
3.1 Viral RNA loads in PBMCs and lymphoid tissue of macaques 18-21 weeks after SHIVC109P7 intra-rectal challenge. 53
3.2 Proviral DNA loads in PBMCs and lymphoid tissue of macaques 21 weeks after initiation of intra-rectal SHIVC109P7 challenges. 57
3.3 Western Blot Results 61
3.4 ELISA 66
3.4.1 Levels of binding Env-gp140 antibody responses in macaque plasma. 66
3.5 Sequencing of the envelope gene from SHIV isolated from different sites in the macaques. 71
Discussion 76
Appendix 84
A. Isolation of Peripheral blood mononuclear cells (PBMCs) from whole blood 84
B. Isolation of mononuclear cells (MNC) from lymph nodes 85
Isolation of MNC from lymph nodes 85
Isolation of splenocytes 85
C. Buffers, Media and Solutions. 86
References 88

PLAGIARISM DECLARATION

This thesis/dissertation has been submitted to the Turnitin module (or equivalent similarity and originality checking software) and I confirm that my supervisor has seen my report and any concerns revealed by such have been resolved with my supervisor.

Name: Kealan Benn

Student number: BNNKEA001

Signature: Signed by candidate

Date: 01/12/2021

DECLARATION

I, Kealan Benn, hereby declare that the work on which this dissertation/thesis is based is my original work (except where acknowledgements indicate otherwise) and that neither the whole work nor any part of it has been, is being, or is to be submitted for another degree in this or any other university.

I empower the university to reproduce for the purpose of research either the whole or any portion of the contents in any manner whatsoever.

Signature: 

Date: 01/12/2021

ACKNOWLEDGEMENTS

To my supervisors, Dr Ros Chapman and Dr Gerald Chege, thank you enough for all the support and encouragement you've given me throughout the duration of my studies. Thank you for your understanding and patience during every challenge I've faced. You have taught me so much in this field and I am very grateful to you.

A special thanks to Craig Adams for training and assisting me for the duration of my studies. For providing encouragement and putting up with me for the duration of my studies.

Thank you to Alana Keyser for assistance in training and preparation of samples. Also, a big thank you for always ensuring that the lab was well stocked

Thank you to CIDRI for the use of your real-time PCR machine.

Thank you to ICGEB for the use of the Versamax plate reader.

Thank you to Professor Anna-Lise Williamson for welcoming me into your lab and group.

Thank you to Professor Carolyn Williamson for the use of the RNA extraction lab and nested PCR room.

Thank you to everyone at PUDAC for your work with the macaques involved in this study.

Thank you to the National Research Foundation (NRF) who has funded my MSc. Degree.

Finally a big thank you to my parents and siblings for supporting me during my masters.

ABBREVIATIONS:

β-ME	Beta-mercaptoethanol
ºC	Degree(s) Celsius
∞	Infinity
µ	Micro
AIDS	Acquired immunodeficiency syndrome.
AGM	African green monkey
ART	Antiretroviral therapy
ARV	Antiretroviral
CCR5	Chemokine receptor 5
cDNA	Complementary DNA
$CD4^+$	Cluster of division 4
ChRM	Chinese Rhesus macaque
CO_2	Carbon dioxide
Cq	Quantification cycle
C_T	Cycle threshold
CXCR4	C-X-C chemokine receptor 4
dH_2O	Distilled water
ddH_2O	Distilled, de-ionized water
DMEM	Dulbecco's modified Eagle medium
DMSO	Dimethyl sulphoxide
DNA	Deoxyribonucleic acid
dNTPs	Deoxytriphosphate
EDTA	Ethylenediamine tetra-acetic acid
eGFP	Enhance green fluorescent protein
ELISA	Enzyme-linked immunosorbent assay
env	Viral gene encoding the envelope protein
Env	Viral envelope protein
ECRA	Ethics Committee for Research in Animals

ESCRT	Endosomal sorting complex required for transport
FAM	6-carboxy-fluorescein
FBS	Foetal bovine serum
FDA	Food and Drug Administration
g	Gram(s)
g	relative centrifugal force
gag	Group-specific antigen
Gp160	160kDa Envelope glycoprotein
Gp120	120kDa Envelope glycoprotein
Gp41	41kDa Envelope glycoprotein
h	Hour(s)
HCl	Hydrochloric acid
HEK	Human embryonic kidney
HIV	Human Immunodeficiency Virus
HRP	Horseradish peroxidase
HVTN	HIV vaccine trials networks
IgG	Immunoglobulin G
IN	Integrase
kb	Kilobases
kDa	Kilodaltons
L	Litre
LTR	Long terminal repeat
m	Milli
M	Molar
MALT	Mucosa-associated lymphoid tissue
$MgCL_2$	Magnesium chloride
min	Minute(s)
mRNA	Messenger RNA
n	Nano
NaCl	Sodium chloride

Nef	Negative Factor
NHP	Non-human primate
Nm	Nanometre
NRTI	Nucleoside reverse transcriptase inhibitors
NNRTI	Non-nucleoside reverse transcriptase inhibitors
OD	Optical density
PBMC	Peripheral blood mononuclear cell
PBS	Phosphate buffered saline
PCR	Polymerase Chain Reaction
pH	Power of Hydrogen
PIC	Pre-integration complex
PNGS	Potential N-glycosylation sites
PR	Protease
qPCR	Quantitative PCR
RNA	Ribonucleic acid
RTC	Reverse transcription complex
rpm	revolutions per minute
s	second(s)
SDS-PAGE electrophoresis	Sodium dodecyl sulphate–polyacrylamide gel
SGA	Single genome amplification
SIV	Simian immunodeficiency virus
TBS	Tris-buffered saline
Th1	T helper type 1
Tris	2-amino-2-(hydroxymethyl)-1,3-propandiol
T/F	Transmitted-Founder
USA	United States of America
V	Volt(s)
vDNA	Viral DNA
VL	Viral load

List of Figures:

Figure 1. 1: HIV structure and genomic organization. 18
Figure 1. 2: HIV replication cycle. 20
Figure 1. 3: Establishment of latently infected $CD4^+$ cells. 30
Figure 2. 1: Schematic diagram showing the timelines of the vaccination regimen and SHIV challenge. 35
Figure 2. 2: DNA sequence showing the region of the SIV gag gene used in the viral load and pro-viral load assays and the primer binding sites 43
Figure 3. 1: RNA viral loads in PBMCs and lymphoid tissue of macaques 21 weeks after initiation of challenges. 55
Figure 3. 2: Comparison of RNA viral loads in vaccinated and control group macaques. 56
Figure 3. 3: Proviral DNA loads in PBMCs and lymphoid tissue of macaques 21 weeks after initiation of challenges. 60
Figure 3. 4: Comparison of Proviral DNA loads in vaccinated and control group macaques. 61
Figure 3. 5: Development of the Western blotting assay. 63
Figure 3. 6: Western Blots for macaques P4 to P72 showing binding antibodies to HIV-1 Env and SIV Gag. 64
Figure 3. 7: Optimisation of a Western blotting assay. 65
Figure 3. 8: ELISA optimization using macaque P38. 67
Figure 3. 9: Graphs showing the change in optical density with serial dilution of plasma from vaccinated macaques at different time points. 68
Figure 3. 10: Endpoint gp140 Env antibody titres to HIV Env for vaccinated macaques 18-21 weeks after the first challenge. 70
Figure 3. 11: Pairwise comparisons showing the percentage similarity and number of differing amino acids in sequences obtained from vaccinated and control group macaques. 73
Figure 3. 12: Amino acid alignment of gp120 sequences from SHIV clones isolated from vaccinated macaques. 74
Figure 3. 13: Amino acid alignment of gp120 sequences from SHIV clones isolated from control macaques. 76

List of Tables:

Table 1 : PCR cycling conditions for TaqMan® RNA-to-C_T™ 1-Step Kit. 41
Table 2: PCR cycling conditions for Proviral DNA assay. 43
Table 3. First round PCR cycling conditions for SGA. 51

ABSTRACT

The development of an effective vaccine against HIV-1 is thought to be a key component of combating the current HIV epidemic. This study aimed to investigate viral reservoirs in the blood and lymphoid tissues after HIV vaccination and virus challenge using the rhesus macaque model. In addition, the study investigated the envelope sequences of the virus located in the potential reservoir sites in an attempt to understand viral variability.

Cryopreserved peripheral blood mononuclear cells (PBMC) and cells isolated from lymphoid tissues obtained at termination of vaccine group (P4, P11, P25, P47, P52) and control group (P67, P70, P71, P72) macaques were processed for determination of viral RNA and proviral DNA loads, and HIV-1 Env amino acid sequences using single genome amplification (SGA) sequencing method. In addition, cryopreserved plasma obtained at key time points pre- and post- vaccination and SHIV challenge were used to measure the levels of HIV Env and SIV Gag antibodies by Western blotting, and HIV-1 Env gp140 ELISA.

RNA viral loads were low for all animals with the median of the averages of the viral load for PBMCs being 3.82 copies/10^7 cells and a range of <1 copies/10^7 cells to 61.15 copies/10^7 cells. For the control group, only P67 had a detectable viral load in the PBMC. The median of the averages for proviral DNA load for PBMCs was 1903.98 copies/10^7 cells and a range of 696.93 copies/10^7 cells to 28 663.88 copies/10^7 cells. Proviral DNA levels were higher than the RNA viral loads indicating a larger amount of integrated provirus and potentially the presence of reservoirs within the macaques. While the low viral load values could mean there are few actively replicating viruses present in the PBMCs. The median of the averages for the RNA viral loads in the inguinal tissue cells was 58.08 copies/10^7 cells with a range of 8.85 copies/10^7 cells to 911.61 copies/10^7 cells. The median of the average for proviral DNA load in the inguinal tissue cells was 3160.36 copies/10^7 cells with a range of 604.67 copies/10^7 cells to 73

140.68 copies/10^7 cells. Proviral DNA levels in the inguinal tissues were higher than the RNA viral load levels which indicates a larger amount of integrated provirus present in the cells of the inguinal tissues and the presence of a potential reservoir. This also indicates that there is less circulating virus.

The Western blots showed that the macaques developed binding antibodies to both HIV Env and SIV Gag, however, non-specific binding of antibodies to proteins other than HIV Env and SIV Gag was also seen. The ELISA effectively showed that both the vaccine group and control group macaques were able to produce binding antibodies. Macaques P4, P47, and P52 had the highest endpoint titre for the vaccine group of 5120. Macaque P71 had the highest overall endpoint titre of 20 480. Macaques P11 and P25 of the vaccine group had an endpoint titre of 1280 which was the same endpoint titre for control group macaques P67 and P70, while macaque P72 had an endpoint titre of 5120.

Single genome amplification and sequencing showed that there were very few amino acid changes between sequences found in macaques. There was minimal variation within the vaccine group and between the vaccine and control groups with amino acid changes in the variable region 1 (V1), glycan N276 in the conserved region 2 (C2) and variable region 4 (V4) resulting in potential N-glycosylation sites (PNGS) being shifted as well as new glycosylation sites being formed while other lost.

This study demonstrates that RNA viral loads and proviral DNA loads were detectable in both macaque groups with no significant difference being present in the viral RNA and proviral DNA loads between the two macaque groups. The lack of changes seen in the sequences of the inguinal and PBMC tissues are due to the early virus seeding the reservoir. Once the reservoir is seeded active replication does not occur in the reservoir resulting in the viruses having similar sequences.

Literature Review

1.1 State of HIV/AIDS epidemic

The HIV-AIDS epidemic while still affecting approximately 40 million people worldwide has seen a decrease in the number of new infections globally. Between 2000 and 2018 the number of new HIV infections globally fell by 37% while global HIV-related deaths fell by 45%, this was largely due to antiretroviral therapy with 13.6 million people being saved due to this intervention (1). Eastern and Southern Africa have played large roles in the global decline in HIV-related deaths as these regions are home to 54% of HIV positive individuals (1). In South Africa, the country with the highest number of new infections, there was a report that indicated a 43% decline in the incidence rate between 2012 and 2017 (2). Despite the decrease in new cases transmission rates are still too high to effectively control the pandemic and there are still those who are infected with the disease and relying on daily medication to keep the virus in check. It is therefore imperative to continue developing preventative as well as therapeutic strategies to deal with this epidemic (2).

Research into vaccines is still ongoing with two main strategies, one being a prophylactic vaccine which is preventative and involves introducing HIV antigens into an uninfected individual with the aim of inducing long-term immunity. The second being a therapeutic vaccine which is not a curative or prophylactic vaccine but is instead designed to decrease HIV replication by strengthening the immune system or possibly creating anti-HIV immunological responses that can supress viral replication below the detection threshold to eliminate the need for antiviral therapy. The development of a vaccine is hindered by the ability of the virus to

quickly establish chronic infections which are difficult to clear, and its ability to rapidly form reservoir sites which enable the virus to avoid current treatment methods (3). Previous HIV vaccine trials have proven insufficient with the humoral and cellular responses elicited from the vaccine providing limited efficacy (4). Despite this limited efficacy, the RV144 human vaccine trial was able to show a statistically significant decrease in the infection risk of HIV. The HVTN 702 trial which was stopped early in 2020 and was deemed safe but not effective and is an example of HIV human vaccine trials which were developed based on the results obtained from the RV144 trial (5).

Currently, the most effective way of controlling HIV infection remains through the use of antiretroviral drugs (ARV) to hinder the replication rates of the virus as no cure exists. The most effective use of these drugs revolves around combinations that target various stages of the replication cycle of HIV (6). Withdrawal of ARVs from patients results in a rebound of plasma viral loads indicating that current drugs are not capable of eradicating all of the virus especially from the reservoirs (7). ARVs target various stages of the replication cycle of HIV. The Food and Drug Administration (FDA) approved the first class of drugs, Nucleoside/Nucleotide Reverse Transcriptase Inhibitors (NRTIs), such as zidovudine. Other drugs approved include Non-Nucleoside Reverse Transcriptase Inhibitors (NNRTIs) such as efavirenz which prevents reverse transcriptase. Other approved drugs include integrase inhibitors such as raltegravir, protease inhibitors such as atazanavir, and entry inhibitors such as ibalizumab. Each of these drugs have different modes of action. Both NRTIs and NNRTIs prevent HIV replication by preventing the reverse transcriptase from transcribing the HIV RNA into DNA (8, 9). Integrase inhibitors block integrase an enzyme which incorporates the HIV DNA into the host genome (10). Protease inhibitors block the protease cleaving Gag and GagPol therefore preventing the maturation of virions (11). Entry inhibitors target the viral entry into host cells, this class of drug is divided into three classes; attachment inhibitors which

prevent the virus from entering $CD4^+$ cells by inhibiting gp120 and $CD4^+$ binding, co-receptor binding inhibitors which prevent viral entry by blocking co-receptor binding, the final entry inhibitor is the fusion inhibitor which prevents fusion of the HIV and host cell membrane therefore preventing HIV from entering the cell (12). These drugs are effective in suppressing the viral loads of these viruses which in turn reduces the likelihood of transmission as well as preventing the emergence of drug resistant variants (13, 14). Despite the ability of ART's to reduce the replication and spread of the virus there is still no consensus as to whether the virus is still capable of replicating despite the treatment, as throughout the treatment very low yet detectable levels of the virus can be detected in the plasma (15, 16). Cell-to-cell spread of the virus is thought to be one of the ways that the virus can spread despite the initiation of ART (17-19).

1.2 Structure and properties of HIV

The genome of the HIV virion contains two identical copies of single-stranded, positive-sense RNA with a size ranging between 9.2 kb and 9.8 kb depending on the HIV type (20). The viral particles of HIV are 120-150 nm in diameter and enclosed by a lipoprotein membrane from which viral glycoprotein spikes protrude. These glycoprotein spikes are composed of trimers of the external gp120 glycoprotein and the transmembrane gp41 protein. The viral envelope encompasses the outer capsid membrane which is formed from the matrix protein p17. Two copies of the HIV viral RNA genome are enclosed within the capsid which is composed of the protein p24. Along with the viral RNA genome integrase, reverse transcriptase and Tat are all located within the virion capsid (21).

The HIV genome (Figure 1.1) is made-up of 9 genes that are responsible for coding 15 different proteins which are synthesized as polyproteins (22, 23). *Gag, pol, and env* are considered the three major HIV genes and code for the structural proteins, viral enzymes, and envelope

proteins. Proviral HIV DNA is generated by reverse transcription of the viral RNA genome into DNA. At either end of the DNA genome long terminal repeat (LTR) sequences are located which contain important regulatory regions. The *gag* gene codes for the matrix protein p17, capsid protein p24 (HIV) or p27 (SIV), nucleocapsid p7 and p6. The *pol* reading frame follows and codes for reverse transcriptase (RT, p51 and p66), integrase (IN p32), and protease (PR, p11). The *env* reading frame which codes for the envelope glycoproteins follows the *pol* reading frame. This reading frame codes for the surface gp120 and transmembrane gp41 subunits (24).

The HIV genome also codes for a number of accessory or regulatory proteins. Transactivator protein (Tat*)* and RNA splicing-regulator (Rev) both play important roles in the initiation of HIV replication (25, 26). Both Tat and Rev stimulate the transcription of proviral DNA into RNA (25-27). Negative regulating factor (Nef*)* may cause the down-regulation of $CD4^+$ from the surface of HIV infected cells and binds to proteins that are involved in pathways that result in the activation of T cells. Nef acts as a virulence factor for HIV and is essential for the spread of the virus as well as disease progression (28). Virus protein r (Vpr) plays an important role in the infection of $CD4^+$ T cells and macrophages, as well as halting cells in the G2 phase, whereby the cell prepares for mitotic division which would occur during the M phase of the cell cycle. Vpr is also an important component of virus particles (29). Virus protein unique (Vpu*)* is important for the budding process as well as the downregulation of $CD4^+$ receptors from the surface of cells (30). Viral infectivity protein (Vif) promotes the degradation of apolipoprotein B mRNA-editing enzyme catalytic polypeptide-like 3G protein (APOBEC3G, A3G) which is responsible for causing guanine-adenine mutations across the viral genome (31). Virus protein x (Vpx*)* which is present in HIV-2 in place of Vpu is critical for viral replication to be able to take place in macrophages (32).

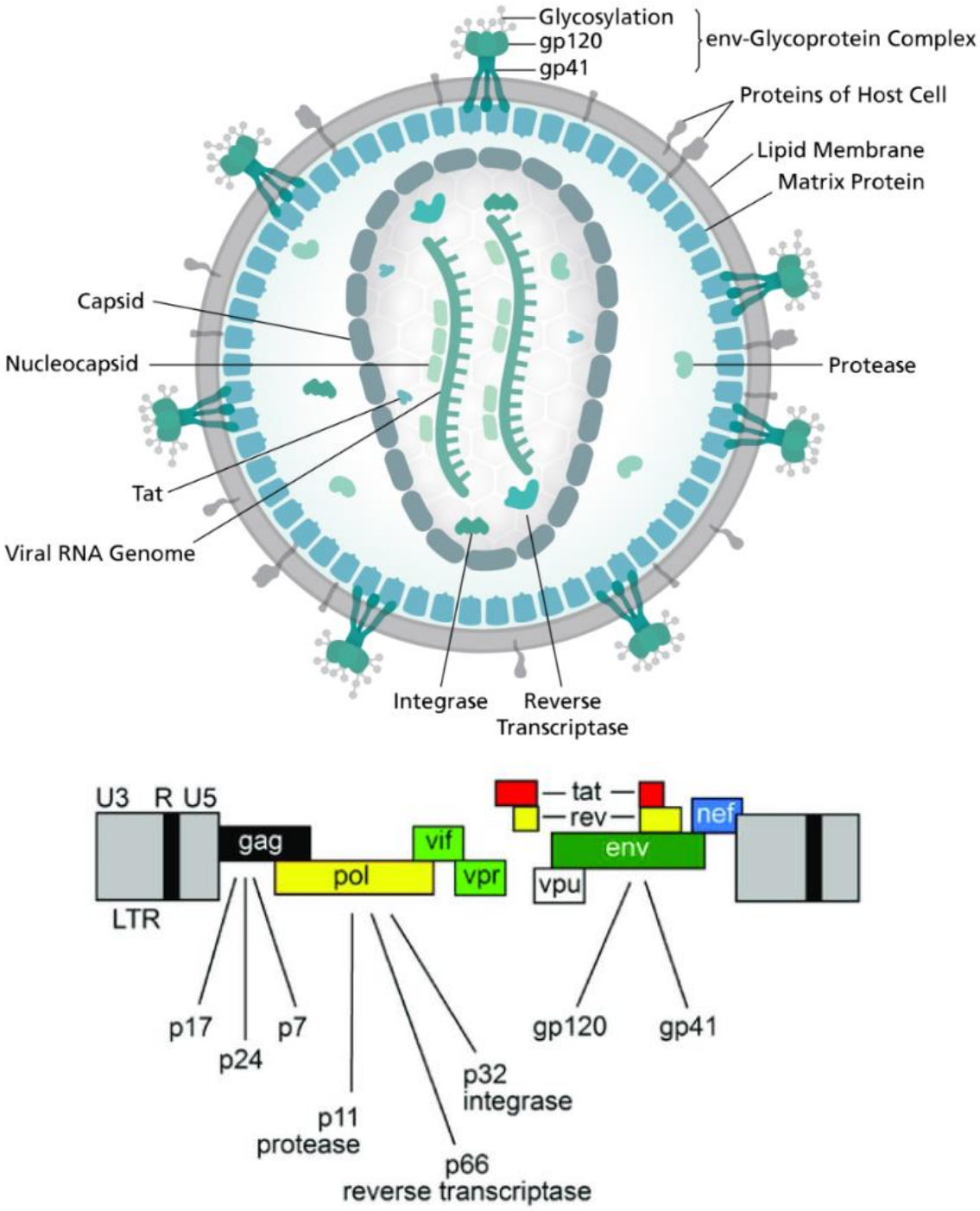

Figure 1. 1: HIV structure and genomic organization.

(A) Structure of an HIV virion. The envelope glycoproteins gp120 and gp41 are present as spikes protruding from the lipid bilayer which originates from the host cell plasma membrane. The gp120 and gp41 form an env-glycoprotein complex. The HIV viral core contains two copies of the HIV viral RNA genome, reverse transcriptase, and integrase encapsulated by the viral capsid protein p24. The contents of the viral core are required for the formation of new virus particles (taken from Thomas Speltstoesser, Wikimedia Commons: https://commons.wikimedia.org/wiki/File:HI-virion-structure_en.svg Accessed 6 March 2021). (**B**) **Genetic organization of the HIV genome.** The proviral genome consists of nine genes which are flanked by long terminal repeats (LTRs; 5' and 3'). The open reading frames code for 15 proteins. The gag gene codes for matrix (MA), capsid (CA) and nucleocapsid (NC) proteins. The

pol gene codes for the enzymes Reverse Transcriptase (RT), Integrase (IN) and Protease (PR). The env gene codes for the envelope glycoproteins gp120 and gp41. The regulatory proteins Tat and Rev as well as the accessory proteins Nef, Vpr, Vpu and Vif are also encoded for [taken from (33)].

1.3 HIV Replication

The HIV replication cycle can be divided into the early and late phases. The early phase represents the events that occur from the moment the virus binds to the surface of the cell up until the integration of the viral DNA into the host cell genome. The late phase encompasses the events that occur from expression of the viral genome to the maturation of new virions (34)

HIV replication begins with the binding of the virus to a cell (Figure 1.2) which it can infect. In order for HIV to be able to infect a cell, the cell needs to express a primary receptor to which the virus can bind. The primary receptor for HIV is cluster of differentiation 4 ($CD4^+$) which is most commonly expressed on T lymphocytes but is also expressed on monocytes, macrophages and dendritic cells. (35). T lymphocytes, monocytes and macrophages are types of white blood cells that are involved in protecting the body from infection (36). Along with the primary receptor HIV requires a co-receptor to initiate infection, this co-receptor is typically either CCR5 or CXCR4 both of which are chemokine receptors. HIV-1 viruses usually use one of the two chemokine receptors with M-tropic or R5 viruses preferentially binding to the CCR5 co-receptor and T-tropic or X4 viruses preferentially binding to the CXCR4 co-receptor. HIV-1 viruses capable of using both co-receptors are termed R5X4 viruses (35). These chemokine receptors are expressed variably among cells. CCR5 is predominantly expressed by memory $CD4^+$ T cells, monocytes, and macrophages whereas CXCR4 is expressed by both memory and naïve $CD4^+$ T cells but at lower levels by monocytes and macrophages (37).

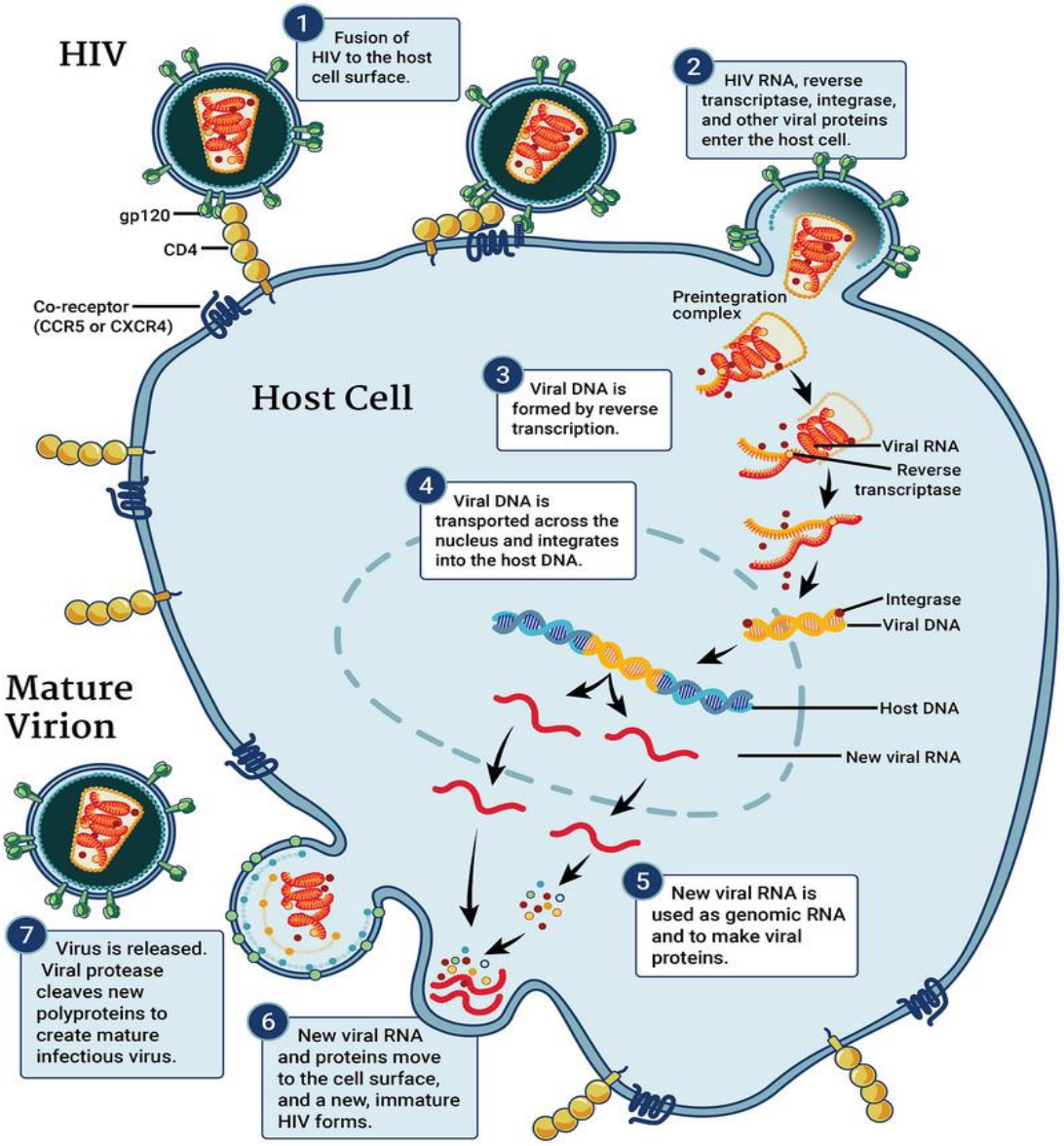

Figure 1. 2: HIV replication cycle.

The HIV replication cycle (1) Binding or attachment. (2) Fusion. (3) Reverse transcription. (4) Integration. (5) Replication and assembly. (6) Budding. (7) Maturation. (Taken from NIAID https://www.niaid.nih.gov/diseases-conditions/hiv-replication-cycle. Accessed 7 March 2021.)

HIV infects susceptible cells by the attachment of the envelope glycoprotein gp120 to the primary receptor $CD4^+$ followed by co-receptor binding. Following co-receptor binding gp120 dissociates from gp41 which undergoes conformational changes that promotes fusion between the viral membrane and the host cell plasma membrane (38-40). Once the membranes have

fused the capsid core is released into the cytoplasm of the host cell. The capsid core at this stage contains the viral RNA, reverse transcriptase, and integrase. Once inside the host cell the capsid core is transformed into the viral reverse transcription complex (RTC) through the uncoating and loss of capsid protein (41). While the virus begins reverse transcription in the RTC soon after entering the host cell, what remains of the capsid core moves toward the cell nucleus by use of the host microtubule network. The viral RNA, which has now been reverse transcribed into linear double-stranded complementary DNA (cDNA), DNA synthesized from a single-stranded RNA template, forms a stable nucleoprotein complex with integrase and other proteins, which is called the pre-integration complex (PIC). Once the PIC enters the nucleus, integrase inserts the viral DNA into the host cell chromosome (42, 43). The integrated viral DNA of the provirus can then be transcribed into mRNA which, with the assistance of host enzymes and machinery, is translated into viral proteins. The 5' long terminal repeat (LTR) has a promoter for viral transcripts located on it, therefore viral transcripts can be expressed with Tat and Vpr both greatly increasing the rate of transcription of viral RNA (44). Initially short completely spliced sections of mRNA are produced which encode for the viral regulatory proteins Tat, Rev and Nef. As mentioned previously Tat activates and enhances viral transcription whereas Rev transports unspliced and incompletely spliced mRNAs encoding the structural proteins, from the nucleus to the cytoplasm, where translation can occur. Nef increases the transcripts being produced and in turn increases viral replication (45, 46). The viral proteins that are synthesized in the cytoplasm can be differentiated into the Gag and GagPol polyprotein precursors, the viral envelope glycoprotein, and the regulatory and accessory viral proteins (39). The viral envelope glycoproteins are synthesized and then trafficked through the rough endoplasmic reticulum, Golgi apparatus and in vesicles to the plasma membrane (34). Envelope glycoproteins are initially synthesized as gp160 a polyprotein precursor in the rough endoplasmic reticulum. In the Golgi, the gp160 is cleaved

by proteases into the surface glycoprotein gp120 and the transmembrane gp41 (47). Simultaneously a 55 kDa precursor Gag protein that forms the virus particle is produced alongside the 160kDa GagPol precursor. The Gag precursor contains the matrix (MA), nucleocapsid (NA) and capsid (CA) domains alternatively the GagPol precursor contains the same domains as Gag with the viral enzyme's reverse transcriptase, integrase and protease included. Once synthesized the Gag along with viral genomic RNA relocates to the plasma membrane of the cell with the aid of the matrix domain of the Gag polyprotein which aids in the integration of the envelope glycoproteins in forming the (48). The capsid domain promotes Gag multimerization during assembly and the nucleocapsid domain aids in recruiting the viral genomic RNA into virions and enables the assembly process. Another domain, the p6 domain, recruits an endosomal sorting complex required for transport (ESCRT) complex which drives the process of budding (34).

Once the immature virion has budded from the host cell, viral proteases cleave the Gag polyprotein to initiate maturation of the virion. The proteases cleave the Gag polyprotein into the matrix protein, capsid protein, nucleocapsid protein, spacer peptide 1 and 2 and p6. These cleaved peptides then rearrange to form the inner viral membrane in the case of the matrix protein, the nucleocapsid forms the nucleocapsid layer which coats the viral genome, and the capsid protein forms the capsid that encompasses the nucleocapsid and the enzymes reverse transcriptase and integrase (49).

During HIV infection the main route of transmission is via the mucosa-associated lymphoid tissue (MALT). These early stages of the infection are driven by M-tropic viruses that infect macrophages, memory T cells, Th1, T cells associated with the intestine, and $CD4^+$ T cells. (36). Soon after infection the virus can exhaust the intestinal T cells expressing CCR5-$CD4^+$. Thereafter there is a large increase in the production of virus and in response T cell proliferation is increased due to the presentation of antigens by infected macrophages, $CD4^+$ T cells, and

dendritic cells. This increase in the production of the virus is termed the acute phase of infection and is followed by the latent phase whereby virus levels in the blood drop in response to $CD8^+$ T cells eliminating large numbers of the infected cells and therefore slowing the virus production. Despite the elimination of infected cells replication of the virus still occurs in lymph nodes and $CD4^+$ T cell numbers continue to decrease. As the disease progresses and $CD4^+$ T cell levels drop to the point whereby $CD8^+$ T cells cannot maintain antiviral measures, the virus levels in the blood begin to rise once again, T-tropic viruses begin to arise, $CD4^+$ T cell numbers begin to decline faster, and the structure of various lymph nodes are altered and ultimately destroyed leading to immune deficiency (36). As the disease progresses mutations can occur which result in a shift from M-tropic to T-tropic viruses. The gp120 of the T-tropic virus binds to $CD4^+$ and the chemokine receptor CXCR4 instead of CCR5.

HIV has quite a low infectivity rate with most infections being transmitted sexually and therefore requiring the virus to penetrate the mucosal barrier for infection to be established. The infection rates are highly variable with multiple factors contributing such as the viral load of the infected individual (50). Despite the large diversity of HIV populations in infected individuals, very few viruses end up establishing a disseminated infection, this phenomenon has been called the transmission bottleneck. This bottleneck in part arises due to immunological and physical conditions that potentially prevent the variants from the infected individual from causing a new infection in the newly infected individual (50). Initially after the transmission of the virus the infection is established in the local tissues at the site of exposure, during this time the virus is undetectable in the systemic circulation (50). Once the virus has disseminated to the lymphoid tissues and throughout the systemic circulation the virus replicates rapidly, during the early stages of virus replication antibody levels are still undetectable (51).

1.4 SHIV

Simian-human immunodeficiency viruses

Simian-human immunodeficiency viruses (SHIVs) are chimeric viruses that contain a SIV genome with HIV-1 *tat, rev, vpu,* and in a majority of SHIVs *env* replacing the SIV *tat, rev,* and *env* genes (52). As SHIV remains capable of infecting macaques it acts as a useful *in vivo* model in the study of the pathogenic properties of the HIV-1 envelope. The majority of the constructed SHIV were developed with genes from HIV-1 subtype B strains which only accounts for approximately 10% of worldwide infections, therefore the available SHIVs are not an accurate reflection of the HIV-1 epidemic which consists predominantly of HIV-1 subtype C virus (53, 54).

Env sequences from HIV-1 variants isolated from chronic or late stages of infection were used to create first generation SHIVs which were not representative of transmitted/founder (T/F) variants as the SHIVs often had CXCR4 tropism instead of CCR5 tropism which is seen in T/F variants. Due to the SHIVs having CXCR4 tropism pathogenesis was altered in the macaques with naïve $CD4^+$ T cells being depleted early during infection (52, 55, 56). To minimize selection *in vitro*, HIV-1 env sequences from CCR5-tropic viruses with a shorter passage history, typically in PBMCs, were used to construct second and third generation SHIVs (56). SHIVs were initially constructed by combining the 5′-half containing gag and pol of SIV, and the 3′-half containing env, tat and rev of HIV-1. To generate these infectious virus particles a transfection is usually performed whereby SHIV DNA is introduced into a cell-line. The culture medium would be changed at a set number of days and the supernatant would be filtered to obtain a virus stock. Finally, the SHIV needs to be adapted to monkey cells through *in vitro* or *in vivo* passaging if the viral infectivity needs to be improved. (57). To determine and

identify whether nucleotide changes occurred during passage the viral genome can be sequenced (53, 57).

A significant issue in the development of subtype C SHIVs was the ability to ensure that the SHIVs were mucosally transmissible and able to cause disease in rhesus macaques. These two issues were vital to overcome to develop effective subtype C SHIVs (54). Some of the SHIVs with HIV-1 subtype C Envs which have been recently produced include SHIV CAP256SU, SHIV-1157, SHIV KB9 C3, SHIVC109P4, and SHIV-327cRM (53-55, 58).

1.5 HIV Immune Responses

In the early stages of HIV infection most individuals lack major symptoms with seroconversion illness being the most commonly experienced (60). Seroconversion illness occurs once the immune system has developed antibodies against HIV. HIV has a rapid rate of replication during the early stages of infection but there is a balance between the replication of the virus and the destruction of immune cells (59, 60). This early stage of HIV infection is called the acute phase during which the HIV viral loads are extremely high increasing the likelihood of potentially infecting another individual. Once an individual has progressed past this initial phase of infection, they usually enter the asymptomatic phase during which no symptoms are present even if the individual is not currently on treatment (61). Despite no symptoms being shown the virus is still taking a toll on the immune system as the virus continues replicating and $CD4^+$ cell counts decrease in response. If treatment is not taken regularly $CD4^+$ counts will continue to fall and with a continuing weakening immune system, the potential of developing symptoms will increase. These symptoms will get progressively worse the longer one goes without treatment and will eventually lead to the development of acquired immunodeficiency

syndrome (AIDS) (60). AIDS usually develops in individuals who have been diagnosed late after having the disease for an extended period. Developing AIDS, however, is not a death sentence. With the correct treatment regimen and healthy lifestyle, individuals can recover, after which they would fall into the category of chronic HIV infection. Chronic HIV infection refers to people who have been on HIV treatment and will continue to take it for the rest of their lives. The treatment keeps the viral load of HIV at a low enough level for the immune system to maintain a relatively stable level, preventing symptoms and opportunistic infections. This stage can last decades (60, 62).

1.6 The HIV-1 envelope protein and its role in immune evasion

HIV-1 contains only one surface protein, Env fusion protein. Glycans compose up to half of this protein's mass, meaning it is heavily glycosylated (63). Glycosylation allows for the release of infectious progeny viral particles and is required for the interaction with host receptors that lead to binding and infection (63). There are low numbers (7-14 spikes per particle) of Env present on the surface of the HIV virion. The scarcity of Env on the virus is associated with its ability to evade the host immune system (64). The scarcity of the spikes present along with the fact that they are unstable results in the shedding of gp120. The trimeric spikes are unstable as the components gp120 and gp41 are non-covalently linked. The shedding of the gp120 proteins leads to the immune system producing antibodies immunodominant non-functional Env forms. The trimeric Env spike has no stable shape, but does have flexibility, with a native closed form that shifts to more open conformations (65).

1.7 Reservoir Formation

HIV often infects the cells of the mucosa-associated lymphoid tissue (MALT) early during infection. The early stages of the infection are driven by M-tropic viruses that infect

macrophages, memory T cells, Th1, T cells associated with the intestine and $CD4^+$ T cells (Figure1.3) (36). Soon after infection the virus can exhaust the intestinal CCR5-expressing $CD4^+$ T cells. Thereafter there is a large increase in the production of the virus and in response T cell proliferation is increased due to the presentation of antigens by infected macrophages, $CD4^+$ T cells and dendritic cells (66). The formation of the reservoir begins with the infection of a $CD4^+$ T cell as it transitions to a resting state. Not much is known about when this occurs during infection, however, reservoirs are present despite early initiation of ART. Presence of the reservoirs can be seen in individuals who start ART within days of diagnosis as the virus rebounds if therapy is halted (68). This implies that the reservoir is formed early and that there is constantly formed prior to the start of therapy (80). The exact timing of the formation of the viral reservoir is not yet determined and studies aimed at determining it are still ongoing (68).

The use of ART is an effective way of halting HIV disease progression by preventing viral replication, however, if ART use is halted the virus is capable of rapidly rebounding. The virus is able to rebound due to its ability to persevere in an infectious state in viral reservoirs (67). The most well understood of the HIV viral reservoirs are resting $CD4^+$ T cells. Before becoming viral reservoirs, these cells are susceptible to infection, it is therefore thought that formation of viral reservoirs are established early during the acute phase of infection after the activated $CD4^+$ T cells have reverted back to a resting state (68). These activated $CD4^+$ T cells have short lifespans due to the cytopathic effects of the virus as well as cytotoxic T lymphocyte-mediated killing (69). If these activated $CD4^+$ T cells survive the cytopathic effects and revert back to the resting state, they become long-lived cells which harbour the integrated HIV provirus which at this time becomes transcriptionally silent but able to produce infectious virus (Figure 1.3) (68).

Viral reservoirs can also be formed when repeated low-dose challenges are used to initiate an infection. Low-dose challenges closely mimic the natural infection while causing disease

without overwhelming the host immune system. Low-dose challenges are preferred to high-dose challenges as high-dose challenges are capable of overwhelming vaccine responses (70). The protective effect of the vaccines is often dependent on the site of vaccination, and the vaccine dosage. Partially protective vaccines are expected to reduce post peak viremia, limit $CD4^+$ T cell loss and prevent progression to AIDS (71, 72). Despite these positive effects, virus can often be detected and isolated in peripheral blood mononuclear cells (PBMCs) as well as in lymphoid tissues such as the spleen, mesenteric and inguinal lymph nodes. (73-75). As the virus can be detected in tissues and blood of animals that have been previously vaccinated and appear healthy it is highly plausible that the virus has formed a reservoir.

One of the primary sites for viral replication are the lymphoid tissues, bone marrow, thymus, and spleen which harbour massive amounts of infected cells. Despite ART being an effective measure to reduce the viral loads in the lymph nodes and spleen, HIV DNA and RNA are still detectable in these tissues years after the initiation of ART (76). These reservoirs are formed due to the inability of current ART to target the latent proviral DNA. It is still unclear whether low-level replication occurs in the presence of ART as drug penetration is not as efficient in these anatomical sites (77). These reservoirs are seeded very early during infection, and it is believed to occur before the symptomatic infection phase occurs and before commercial assays can confirm infection. Despite the early seeding of viral reservoirs, early ART can limit the size of the viral reservoir (67, 69). It remains a challenge to detect the stage at which HIV potentially forms a reservoir in humans since we are currently unable to detect the virus at the earliest stages of infection as the current methods of detection rely on the systemic viremia phase (69). However, work has been done to determine the potential time window where a stable reservoir can form in individuals who are on ARV drugs (78). In rhesus macaques, however, viral rebound, with persistent detectable virus levels, could be seen even after initiation of ART before systemic viremia occurred. Further studies on macaques have shown

that 1-3 days post infection SIV-DNA can be detected in tissues at the portal site of entry before systemic viremia occurs (69, 76). During this early stage of infection, the virus actively infects resting $CD4^+$ T cells (70). Resting $CD4^+$ T cells are present in more significant numbers than other target cells, increasing the probability of this cell being infected. An influx of activated CD4+ cells occurs when the immune system is stimulated (70). These cells then are infected, leading to further dissemination of the virus. (69).

SIV and SHIV reservoirs are found in infected macaques, with most of the viruses being unable to replicate; this is also seen in people living with HIV-AIDS, however the percentage of defective SIV or SHIV is lower than in people living with HIV-AIDS (79). Bender *et al* determined that only 28% of SIV and 15% of SHIV sequences were intact when compared to 1-10% for HIV reservoirs (80). Despite there being a larger number of intact SIV and SHIV proviruses in infected macaques when compared to humans infected with HIV, these proviruses do not make up a majority of the sequences present in the reservoir of the macaques (79). Similar to people living with HIV-AIDS there can be a variation in the viral DNA (vDNA) present in peripheral blood mononuclear cells (PBMCs), lymphoid tissues and the gastrointestinal tract (81). The PBMCs, lymphoid tissues and gastrointestinal tract usually contain the highest levels of vDNA while inversely the tissues of the lung, brain and bone marrow usually contain the lowest vDNA levels (81).

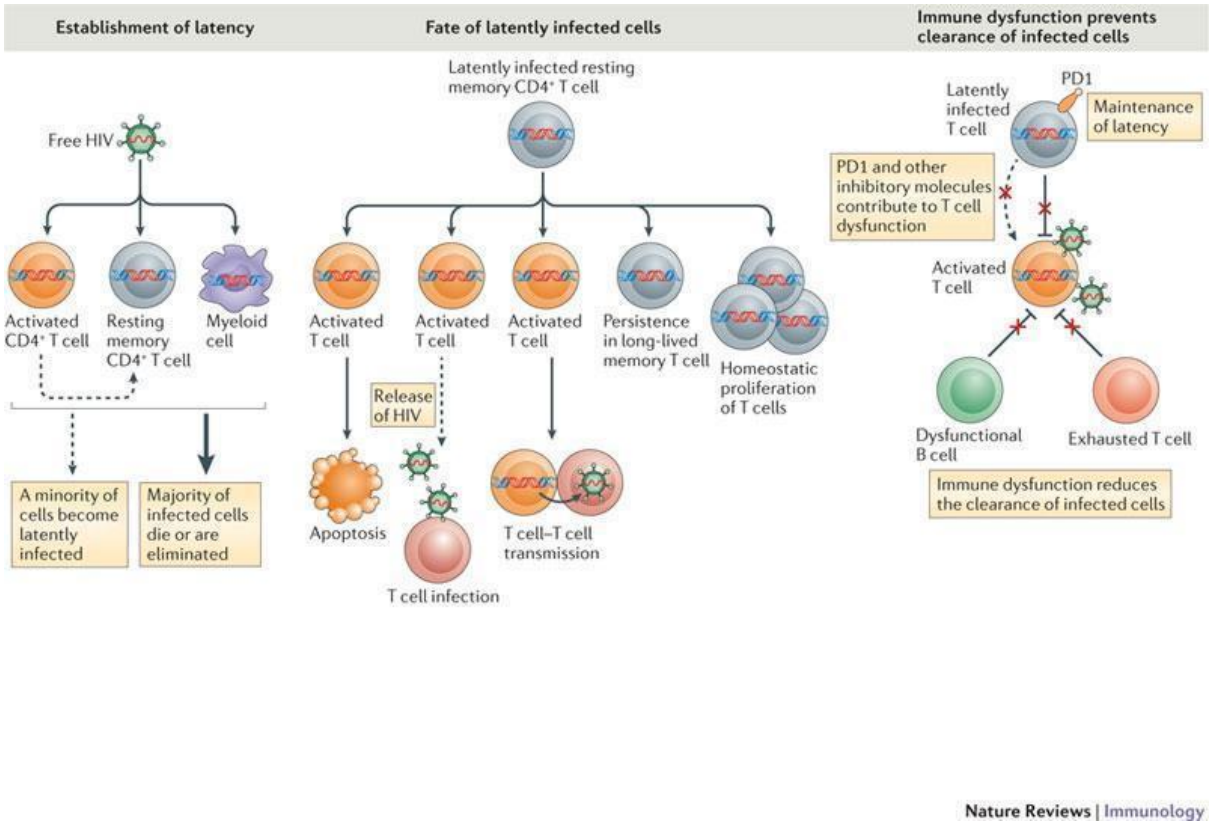

Figure 1. 3: Establishment of latently infected CD4$^+$ cells.
This image illustrates how latent HIV infection can be established in T cell and myeloid cells. A majority of infected cells die, a few are capable however of reverting to a resting state. Once latently infected these cells can either die, become new infection sources, which survive as long-lived cells, or the cells can expand through homeostatic proliferation (taken from (82)).

1.8 Nonhuman primate models to test HIV vaccine candidates.

The ideal nonhuman primate (NHP) model would be one where a NHP could be infected with HIV-1 and cause an AIDS-like syndrome similar to what is seen in humans. Very few NHPs can be infected with HIV-1. These include the chimpanzee, gibbon ape and pig-tailed macaque. Despite these NHP being capable of being infected with HIV there is a poor progression to AIDS. The chimpanzee and gibbon ape are both protected species and are not available for research (72, 83).

Various species of African monkeys are natural hosts of SIV, but they do not develop signs of disease once infected. Asian monkeys however, when infected with certain strains present with

high viral loads, $CD4^+$ T cell depletion, and opportunistic infections (84). There are three main species of macaques: rhesus macaques, pig-tailed macaques and cynomolgus macaques. Of the three mentioned species, rhesus macaques are most frequently used, with the Chinese origin and Indian origin sub-species most often used in NHP models. Indian rhesus macaques are more established as a model but there is currently a global shortage of this sub-species whereas the Chinese rhesus macaques are readily available (85). SIV infections vary between these macaques as well with SIV and SHIV infection progressing slower in Chinese macaques compared to Indian macaques (86).

The rhesus macaque monkey is used as the preferred model of choice in most animal experiments involving HIV research as these monkeys share features present in people infected with HIV-AIDS such as anatomy, physiology, immune system, infectious agents, and susceptibility to antiretroviral treatments. As these monkeys are relatively large, they are also able to be sampled frequently (87). Despite these monkeys being the preferred model, HIV does not infect macaques, therefore SIV or SHIV are used for challenge experiments as they can cause symptoms similar to those that are present in people infected with HIV-AIDS. African monkeys such as the African green monkey (AGM) do not develop AIDS symptoms when infected with SIV despite developing persistent viraemia with high viral loads. AGMs are still useful in the study of natural resistance to HIV disease progression (86). Macaques infected with SIV show all the biological features of HIV infection meaning that this model is ideal for the testing of therapeutic strategies aimed at disrupting the pathogenesis of HIV and normalization of chronic inflammation and immune activation. AGM plays a vital role in the understanding of how chronic immune activation and inflammation drive disease progression. The natural hosts of SIV are also able to maintain their mucosal barrier. By artificially increasing immune activation and inflammation in these monkeys scientists were able to

determine that immune activation and inflammation were key drivers of disease progression (88).

Rhesus macaques are an important model for drug evaluation and vaccine research as the progression of disease is so similar to that of humans furthermore these macaques develop tuberculosis and other diseases that are similar to humans infected with HIV (89). SIV is a suitable substitute for HIV in these studies as the viruses share key pathogenic features such as integration into the host genome and the distribution of infected cells is similar in both humans and the non-human primates (84, 86, 87, 90-92).

1.9 Project Rationale

As research into HIV cures continues further understanding of viral reservoirs is still required. Viral reservoirs have been a major impediment to both HIV treatment and drug development. By obtaining a greater understanding of these latent viral reservoirs, drug development could be streamlined in the future to target these areas which harbour the virus. There has been a shift in focus towards the development of therapeutics to control virus expression and potentially eliminate the virus. Also, there is currently a lack of knowledge as to whether partially protective HIV vaccines impact on the sizes of viral reservoirs after break-through infections. A partially protective HIV vaccine could still be useful in reducing the peak and set-point viral loads and thus potentially delaying progress to disease. In a previous unpublished HIV vaccine study by our research group, a group of six NHP were vaccinated with candidate vaccines and subsequently challenged intrarectally with a SHIV inoculum while a control group of four NHP was unvaccinated but challenged in an identical manner. The vaccination regimen was not protective, and all the animals got infected, thus offering an opportunity to study the vaccine effect on viral reservoirs. The challenge virus SHIV109P7

used in this experiment was derived from SHIVC109F.PB4, a molecular clone from an infected individual in Zambia that expressed the soluble-$CD4^+$ ($sCD4^+$)-sensitive CCR5-tropic clade C envelope (93). Therefore, this study sought to investigate the peripheral blood and various lymphoid sites and determine the sizes of SHIV reservoirs in Chinese rhesus macaques at the time of termination to assess whether vaccination had any effect on the size and location of these reservoirs. The study further sought to characterise the viral variants in the blood and various lymphoid tissues to determine if they were different. Finally this study sought to determine whether Env-binding antibodies were developed in the macaques as they have the potential to contribute to protection against SIV in macaques as well as viral control.

1.10 Aims.

This study aims to determine the sizes of SHIV reservoirs present in Chinese rhesus macaques. The objectives are as follows:

Objective 1: to quantify SHIV reservoirs in the blood and different lymphoid tissues from vaccinated and unvaccinated (control group) rhesus macaques.

Objective 2: To characterize the viruses in the different lymphoid tissues and blood by single genome amplification (SGA) and Env sequence analysis.

Objective 3: To determine if the macaques developed binding antibodies to SHIV Env and Gag antigens.

Materials and Methods

2.1 Background information of samples used in the study.

2.1.1 Biological samples used in this study.

The biological samples used in this study were obtained from Chinese-origin rhesus macaques (ChRM) which were used in a previous unpublished study done by our research group. The animals were divided into two groups, the vaccine group which consisted of 6 monkeys and a control group which consisted of 4 monkeys (Figure 2.1). Animals were challenged until they were successfully infected, of the vaccinated animals P25 got infected after a single challenge at week 32, P4, P11, P47 and P52 after two challenges at weeks 32 and 33 and P38 required four challenges at weeks 32 to 35. To become infected, P70 and P72 of the control animals were challenged twice at weeks 32 and 33, P71 was challenged three times from week 32 to 34 and the final control animal P67 was challenged four times from week 32 to 35 (Figure 2.1). The samples were sourced from cryo-preserved plasma, peripheral blood mononuclear cells (PBMC) and cells isolated from inguinal, mesenteric, and axillary lymph nodes as well as the spleen (Appendix A-B). Plasma samples were stored at -20°C whereas PBMC and cells isolated from inguinal, mesenteric, axillary lymph nodes and spleen were stored in liquid nitrogen (at <-180°C).

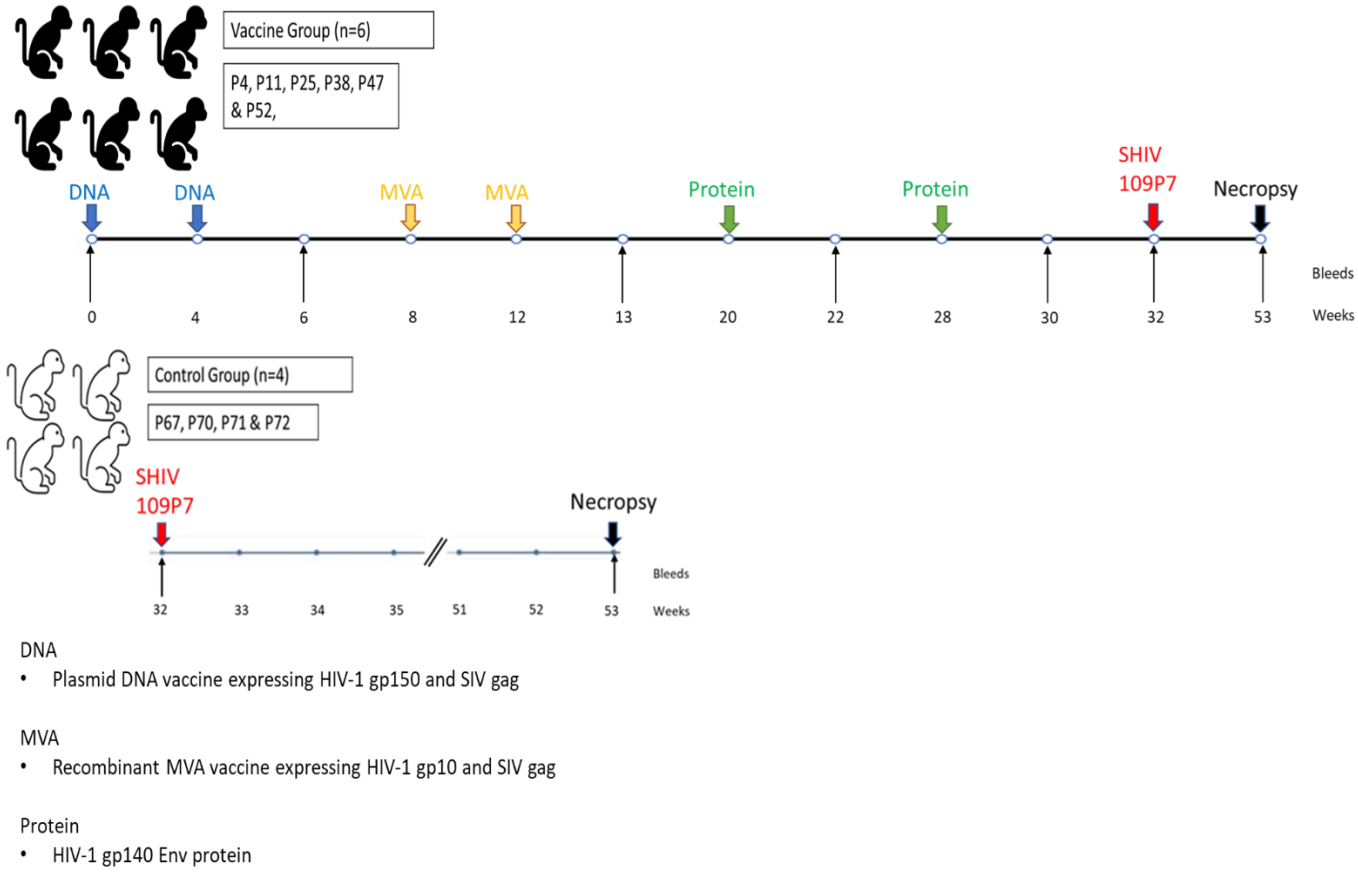

Figure 2. 1: Schematic diagram showing the timelines of the vaccination regimen and SHIV challenge.

The animal identification numbers are indicated below each group. The vaccine group animals received the vaccination regimen at weeks 0, 4, 8, 12, 20 and 28 as indicated by downward arrows. Both the vaccine and the control groups were challenged weekly with SHIV via the intra-rectal route starting at week 32 until viraemia was confirmed. The DNA and MVA vaccines expressed SIV Gag and HIV-1 gp150 envelope. The HIV-1 envelope amino acid sequence was derived from the sequence of the Env of SHIVC109P7 that had been adapted to ChRM by a rapid 3-step *in vivo* serial passage (94). The same envelope was used to generate the soluble gp140 protein vaccine. Necropsies for both groups of animals occurred at week 53 except for P38 which was delayed by 2 months. Cryo-preserved samples that were used in the current study were obtained at weeks 0, 6, 13, 22, 30, 32 and 53 as indicated with upward arrows.

2.1.2 Information on experimental animals from which samples were derived.

No ethical clearance was required for the current study as only cryo-preserved biological samples were used. However, the original study from which these samples were obtained was approved by both the Ethics Committee for Research in Animals (ECRA) of the South African Medical Research Council (ECRA Ref: 06/14) and the Health Science Faculty Animal Ethics Committee (HSFAEC) of UCT (HSF AEC Ref: 014/044).

2.1.3 Preparation of samples and acknowledgements

Preparation of samples was done by Alana Keyser, Craig Adams, and Dr Gerald Chege. Plasma, PBMCs and cells from lymphoid tissues were prepared as described in the Appendix A-B. Separated plasma was then aliquoted and stored at -20 ℃ whereas the isolated PBMCs and cells from lymphoid tissues were stored in liquid nitrogen. Samples were cryo-persevered for approximately 1-2 years prior to use in this experiment.

2.2 DNA and RNA Extraction from PBMCs and splenocytes and lymphoid cells.

DNA was extracted from PBMCs, splenocytes and cells isolated from inguinal and mesenteric lymph nodes to determine the amount of integrated provirus in peripheral blood and lymphoid tissues. Likewise, RNA was extracted from the same cells in order to determine the viral loads within those sites. Extracted RNA was also used to synthesise cDNA that was used for the single genome amplification and envelope sequencing procedures described later.

DNA and RNA were simultaneously extracted from the PBMCs, splenocytes, mesenteric cells and inguinal cells of the macaques according to instructions provided in the ALLprep DNA/RNA kit (QIAGEN). Cryopreserved samples of PBMCs, splenocytes and cells extracted from inguinal and mesenteric lymph nodes were thawed, diluted in R10 media (RPMI medium 1640 (GIBCO/Invitrogen), 10% fetal bovine serum (FBS), 100 U/mL penicillin, and 100 µg/mL streptavidin). The cells were then pelleted by centrifugation for 10 minutes at 250 *g*. The pellets were retained and resuspended in 600 µL of Buffer RLT Plus containing 10 µL of β-mercaptoethanol (β-ME) per 1 mL of Buffer RLT Plus. β-ME is added as it acts to irreversibly denature RNases which degrade RNA (95). The resulting lysate was then added to a QIAshredder spin column (QIAGEN) placed in a collection tube and centrifuged at maximum speed for 2 minutes to homogenise the lysate. The homogenized lysate was then transferred into an AllPrep DNA spin column (Qiagen) placed in a clean 2 mL collection tube and centrifuged for 30 seconds at 8000 *g*. During this step genomic DNA was bound to the AllPrep DNA spin column and RNA purification proceeds with the flow-through. The AllPrep DNA spin column which now contained bound genomic DNA was placed in a clean 2 mL collection tube and stored at 4°C for later purification as RNA tends to be less stable than DNA. While the DNA spin column was stored at 4°C, RNA purification proceeded. One volume (600 µL) of 70% ethanol was added to the flow-through to provide favourable binding conditions for the RNA. The flow-through obtained by spinning the homogenized lysate through the AllPrep DNA spin column was mixed well by pipetting and seven microlitres of this sample was added to a RNeasy spin column (QIAGEN) placed in a 2 mL collection tube before centrifuging for 15 seconds at ≥8000 *g*. The flow-through was then discarded, and this step was repeated using the same column and the remainder of the sample. During this step RNA is bound to the spin column. Following this step, the spin column is washed with Buffer RW1 (Qiagen), which removes molecules that have non-specifically bound to the spin column such as carbohydrates,

proteins, and fatty acids, the column is centrifuged for 15 seconds at 8000 *g* after which the flow-through is discarded. A further wash with Buffer RPE (Qiagen), which removed salts attached to the column from previous buffers, is performed where the spin column is centrifuged for 15 seconds at 8000 *g*. After the centrifugation, the flow-through was discarded and the wash with Buffer RW1 (Qiagen) was repeated in the same spin column and centrifuged for 2 minutes at 8000 *g* to ensure that no ethanol is present in the remaining steps. Following the washes, the RNeasy spin column was placed in a clean collection tube and centrifuged for 2 minutes at maximum speed in order to remove any excess buffer or ethanol present in or on the spin column. This step is essential in obtaining a clean eluate. The final step in RNA purification was to elute the sample; the RNA spin column was placed in a new 1.5 mL collection and 50 μL of RNase-free water was added to the spin column. The samples are then allowed to incubate for 5 minutes to increase the yield, following this 5-minute incubation the samples are centrifuged for 1 minute at 8000 *g* to elute the RNA. The RNA samples were then stored for later use in the viral load assay as well as for cDNA synthesis at -80°C. Once the RNA samples are stored safely DNA purification can commence by washing the AllPrep DNA spin column with 500 μL of Buffer AW1 (Qiagen) and centrifuged for 15 seconds at 8000 *g*. The second wash follows the discarding the flow-through, with 500 μL of Buffer AW2 (Qiagen) added to the spin column which was then centrifuged for 2 minutes at 8000 *g*. The DNA washes serve a similar purpose as the washes in the RNA purification protocol, by actively removing contaminating proteins, lipopolysaccharides and small RNAs to increase the purity while the DNA remains bound to the membrane. Following the washes, the AllPrep DNA spin column was placed in a clean collection tube and centrifuged for 2 minutes at maximum speed in order to remove any excess buffer or ethanol present on or outside of the spin column as any residual ethanol can interfere with downstream reactions. To elute the DNA, the spin column was placed in a clean 1.5 mL collection tube and 100 μL of Buffer EB

added to the spin column, followed by a 5 minute incubation at room temperature before a centrifugation at 8000 *g* for 1 minute to elute the DNA. The DNA was stored at -80°C for later use in the proviral DNA assay.

2.3 Measurement of RNA and DNA levels in tissues

Real-time PCR (quantitative PCR, qPCR) can be conducted due to the ability to monitor DNA amplification in real time by monitoring fluorescent activity. This fluorescent activity can be measured after the individual cycles during the PCR and gives an indication of the amount of DNA amplicons present in the sample (96). The intensity of the fluorescent signal can be measured. During the initial phases of PCR the intensity of the fluorescence should be minimal and indistinguishable from the background fluorescence (97). As more cycles are completed however, the intensity of the fluorescence could increase. Once the signal can be detected above the background, we reach a point called the quantification cycle [also referred to as cycle threshold (C_T)] which is the point at which DNA quantity can start being determined with the use of a standard curve (96).

TaqMan® probes contain a reporter dye such as 6-carboxy-fluorescein (FAM) which is linked to the 5' end of the probe, and a nonfluorescent quencher which is located at the 3' end of the probe. Quencher molecules quench the fluorescence emitted by the reporter molecule. During the PCR process once the template separates into two strands and the thermocycler cools, the probe which is labelled with both the reporter and quencher molecules and primers which are sequence-specific, are able to anneal to the single stranded templates. During the extension of the templates polymerase, such as DNA polymerase, displaces the reporter and quencher molecule from the probe which results in fluorescence (98, 99).

2.3.1 RNA viral load assay

The RNA viral load assay was used to determine SHIV viral loads, that is the number of copies of SIV gag RNA in 10 million cells, in cryopreserved cell samples of macaques. The primers and the probe used were obtained from Biosearch Technologies. The sequence for the forward and reverse primers are: PDGAGF 5' GTCTGCGTCATCTGGTGCATTC 3' and PDGAGR 5' CACTAGGTGTCTCTGCACTATCTGTTTTG 3' respectively. The probe (PDGAGP) had a sequence of 5' FAM-CTTCCTCAGTGTGTTTCACTTTCTCTTCTGCG-BHQ-1 3'. The master mix was made up using the TaqMan® RNA-to-C_T ™ 1-Step Kit (Qiagen) as follows: 1X Taqman RT-PCR mix, 1X Taqman RT enzyme mix, 0.4 µM PDGAGF (forward primer), 0.4 µM PDGAGR (reverse primer), 0.1 µM PDGAGP (TaqMan probe). The plate was stored on ice while the SIV *gag* RNA standard (Resource of Nonhuman Primate Immune Reagents, Emory University) was serially diluted down 100-fold to obtain a range of 10^0 – 10^8 *gag* copies/mL. The standard was serially diluted by adding 1 µL of the 10^{10} stock to 99 µL of nuclease free water, this was repeated until 10^0 *gag* copies/mL was obtained. One microlitre of the template, either the RNA standards or RNA sample was then added to the plate which was sealed with adhesive film and placed on ice. One microlitre of the positive control, RNA from a SHIV-infected macaque, and the negative control, RNA from an uninfected macaque, were also added to their respective wells prior to the plate being sealed and placed on ice. The PCR was run on a QuantStudio 7 Real-time machine (Applied Biosystems) in triplicate according to the cycling conditions for the TaqMan® RNA-to-C_T™ 1-Step kit (QIAGEN) as indicated in Table 1. Viral RNA levels were determined from a standard curve of known concentrations of SIV *gag*, with a range of 10^0 to 10^8 *gag* copies, to obtain gag copies per 10^7 cells used. The standard curve was created using a SIV *gag* RNA stock (Yerkes National Primate Research

Center, Emory University, Atlanta, Georgia, USA) and the data was expressed as SIV gag RNA copies per 10^7 cells.

Table 1 : PCR cycling conditions for TaqMan® RNA-to-C_T™ 1-Step Kit.

Stage	Step	Temperature	Time
Holding	Reverse transcription	48°C	15 minutes
Holding	Activation of DNA polymerase	95°C	10 minutes
Cycling (40 cycles)	Denature	95°C	15 seconds
	Anneal/Extend	60°C	1 minute

2.3.2 Proviral DNA Assay

The proviral DNA assay was used to determine the amount of proviral DNA (integrated SHIV DNA) present in PBMC, splenocytes and cells isolated from the inguinal and mesenteric lymph nodes between vaccinated and unvaccinated macaques. A SIV *gag* DNA standard was obtained from Craig Adams, the primers for the *gag* region of SIV used as the standard are shown in Figure 2.2 The standard was constructed by amplifying the *gag* gene from SHIVC109P4 using PCR after which it was cloned into the pMiniT vector. Five-fold serial dilutions of the plasmid DNA standard were made to obtain a range of 3.2 to 50 000 copies per mL. Nine microlitres of the master-mix, 1X Taqman gene expression master mix, 0.4 µM PDGAGF (forward primer), 0.4 µM PDGAGR (reverse primer), 0.1 µM PDGAGP (TaqMan probe), were dispensed per well of a MicroAmp™ Optical 384-Well Reaction Plate (Thermofisher). The

same probe and primers were used for both the proviral DNA assay and the RNA viral load assay as the same region of *gag* was used. The main difference between the two assays was the usage of TaqMan® RNA-to-C_T^{TM} in the RNA viral load assay as the template initially used was RNA that needed to be reverse transcribed; the proviral DNA assay used a DNA template therefore the Taqman Gene Expression Mastermix (Qiagen) was used. One microlitre of the template, either the DNA standards or DNA sample, was then added to the plate which was then sealed with adhesive film and placed on ice. One microlitre of the positive control, DNA extracted from an infected macaque, and the negative control, DNA extracted from an uninfected macaque, were also added to their own wells prior to the plate being sealed and placed on ice. The PCR was run on a QuantStudio 7 Real-time machine (Applied Biosystems) according to the cycling conditions listed in Table 2. Proviral DNA levels were determined from a standard curve of plasmid DNA and the data was expressed as SIV *gag* DNA copies per 10^7 cells.

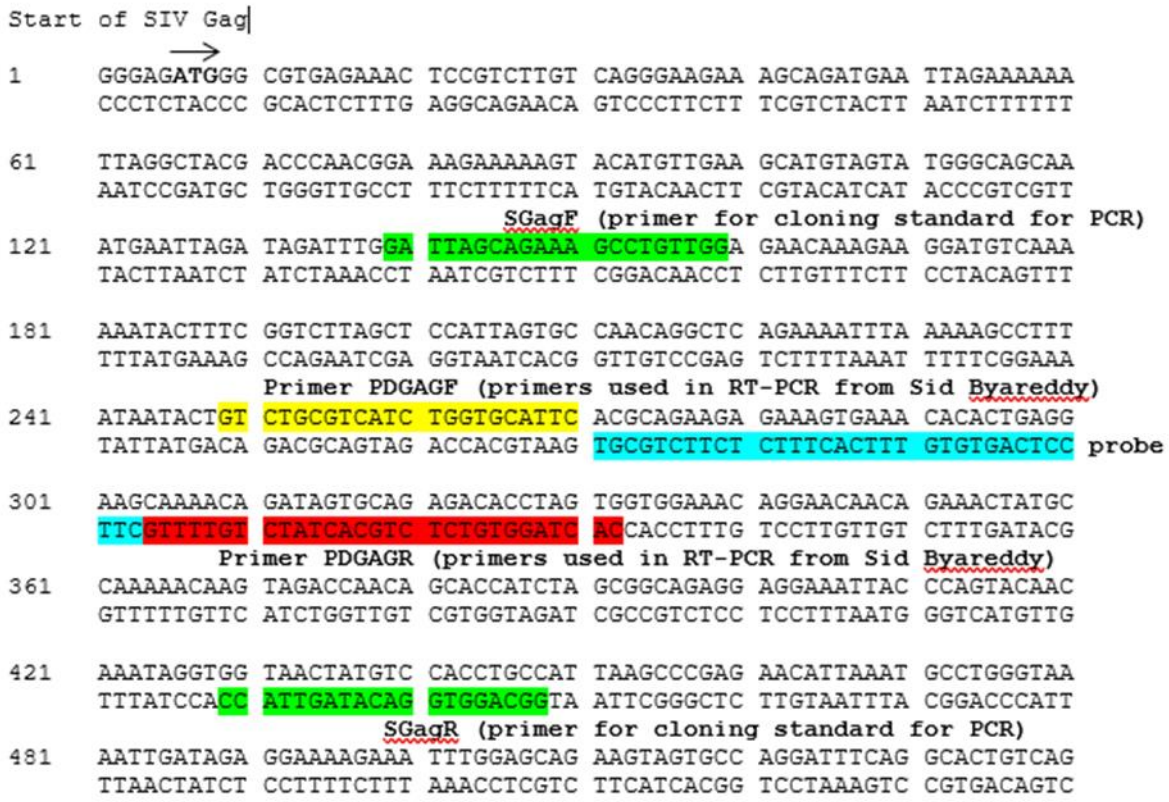

Figure 2. 2: DNA sequence showing the region of the SIV *gag* gene used in the viral load and pro-viral load assays and the primer binding sites:
The yellow-shaded primer (PDGAGF) and the red-shaded primer (PDGAGR), with the blue-shaded probe were used in a Real-time PCR assay (viral load assay) to determine viral loads, as described by (Baba et al., 2000). The green—shaded primer pairs (SGagF and SGagR) were used to generate the cloned DNA standard in the adapted RT-PCR proviral assay to measure DNA levels.

Table 2: PCR cycling conditions for Proviral DNA assay.

Stage	**Step**	**Temperature**	**Time**
Holding	Initialisation Step	50°C	2 minutes
Holding	Activation of DNA polymerase	95°C	10 minutes
Cycling (40 cycles)	Denature	95°C	15 seconds
	Anneal/Extend	60°C	1 minute

2.4 Preparation of cell lysates from cells infected with modified vaccinia Ankara (MVA) expressing HIV-1 Env and SIV Gag for Western blotting.

2.4.1 Infection and subsequent harvesting of lysates from HEK293T cells infected with MVA expressing HIV-1 Env and SIV Gag

SIV Gag and HIV-1 Env proteins for Western blotting were obtained by infecting HEK293T cells with a recombinant MVA that expressed these antigens (MVA-109P4) and preparing cell lysates that were then separated by SDS-PAGE and transferred to a membrane. The membrane was then probed with macaque sera to determine if there were binding antibodies to SIV Gag and HIV-1 Env present.

To obtain the cell lysates, two 6-well tissue culture plates were seeded at $0.2x10^6$ HEK293T cells/mL in a total volume of 2 mL of Dulbecco's Modified Eagle Medium (DMEM) and incubated for 24 hours at 37°C and 5% CO_2. The cells, which were approximately 80% confluent, were then infected, after media removal, with either 500 µL of MVA-109P4 or 500 µL wild type MVA at a multiplicity of infection (MOI) of 0.2 and then incubated for a further two hours after which 1.5 mL of DMEM was added to each well. The 6-well plates were then incubated for a further 48 hours. MVA-109P4 contained the green fluorescent marker (eGFP) which was used to visualize gene expression and confirm infection using a fluorescent microscope. Following confirmation of eGFP expression, 200 µL of 1X Glo Lysis Buffer (Promega) was added to the individual wells to lyse the cells. The cell lysate was then spun at 4°C for 10 minutes at 13 000 rpm. The cell lysate was then stored at -20°C for further use.

2.4.2 Western Blot assay

An in-house Western blotting procedure was developed to confirm whether the macaques had developed antibodies to HIV-1 Env and SIV Gag contained in the vaccines and the SHIV challenge viruses. Antigens generated by infecting HEK293T cells with recombinant MVA expressing *gag* and *env*, were validated to be Gag and Env-specific by probing with commercial anti-Gag and anti-Env antibodies. This validation was followed by determining the optimal plasma dilution to use to obtain blots with minimal background and visible bands of interests. In the assay, proteins in the cell lysates generated above were separated by sodium dodecyl-sulfate polyacrylamide gel electrophoresis (SDS PAGE) according to their molecular weight, transferred onto polyvinylidene fluoride (PVDF) membranes which have a high protein affinity, and probed with macaque plasma, followed by incubation with a secondary antibody conjugated to alkaline-phosphatase, and detected with substrate. The assay was a qualitative and not a quantitative assay confirming the presence of antibodies to HIV-1 Env and SIV Gag. Eight percent resolving and 4% stacking gels were used for the SDS PAGE (Appendix C). The BioRad MiniPROTEAN® Tetra Handcast system was used to cast the gels and the BioRad MiniPROTEAN® Tetra Vertical Electrophoresis system was used for electrophoresis. Fifteen microlitres of the cell lysate was mixed with a 4X Laemmli buffer and equivalent amounts of this lysate was loaded into each well. Precision Plus Protein Dual Color Standards (Bio-Rad) was used as a marker to size the protein bands. The gels were electrophoresed at a constant voltage of 200 V for one hour. The PVDF membrane was soaked in 100% methanol for 30 seconds in order to activate the membrane and then placed in Transfer Buffer for 5 minutes to equilibrate it. Proteins were transferred to the treated PVDF membrane by electroblotting at 25 V for one hour.

After transfer, the PVDF membrane was removed from between the blotting sheets and stained with Ponceau S dye for two minutes, followed by rinsing with distilled water until band visualisation. Ponceau S (Appendix C) staining had a dual function of determining transfer

efficiency as well as in aiding in protein band visualisation for the cutting of the membrane into strips according to the wells. The strips were then placed in Blocking Buffer (Appendix C) at 4°C overnight without shaking, to prevent the non-specific binding of antibodies to the membrane. The blocking buffer was replaced with varying dilutions of macaque plasma and incubated for two hours at room temperature with gentle shaking. Three dilutions of macaque plasma, 1:100, 1:200 and 1:500 diluted in blocking buffer, were tested to determine the optimal dilution for Westerns.

Preliminary plasma dilution optimisation was followed by pre-absorption of macaque plasma, to further reduce background. This was performed by incubating wild type MVA-infected HEK293T cell lysate with macaque plasma prior to incubation with the strips in order to reduce nonspecific binding of antibodies to proteins other than the antigen. The pre-absorption was performed by incubating 1 mL of the plasma with 5 mL of the supernatant of the cell lysate of the HEK293T cells infected with wild type MVA, overnight at 4°C with shaking. The MVA vaccine is likely to have induced the generation of antibodies to the MVA vector itself. Pre-absorption was intended to allow the anti-MVA antibodies in the plasma to bind to their corresponding proteins in the cell lysate before incubating the plasma with the blots.

The strips were washed with shaking at room temperature four times for fifteen minutes with Blocking Buffer following the incubation with the macaque plasma. Anti-monkey IgG secondary alkaline-phosphatase antibody (Sigma) was diluted 1:10000 in blocking buffer and incubated with the PVDF strips for two hours while shaking. Following the incubation, the antibody was removed, and the membranes were washed four times with Blocking Buffer for fifteen minutes with shaking. After the wash step the Blocking Buffer was removed and 5 mL of 5-bromo-4-chloro-3-indolyl phosphate/nitro blue tetrazolium substrate (NBT/BCIP) was added to the membranes. The membranes were then placed in the dark until bands were visible. The band visualisation reaction was stopped by rinsing the membrane with reverse osmosis

purified water. The membranes were then dried overnight. Images of the Western blots were taken using a ChemiDoc XRS+ System (Bio-Rad). The Western blots were analysed by comparing the size of the bands of Env 155 kDa and Gag 55 kDa as well as the banding patterns to controls.

2.5 HIV envelope ELISA

Enzyme-linked immunosorbent assays (ELISA) is an immunological assay used to detect and measure concentrations of solutes such as antibodies, antigens, peptides, and cytokines present in a test sample. The test solute is captured and immobilized on the surface of a microwell plate. Once bound to the surface, a primary antibody is added which could be either conjugated or unconjugated. If the antibody is conjugated to an enzyme such as horse-radish peroxidase (HRP) or alkaline phosphatase it is known as a direct ELISA. If the primary antibody is not conjugated a secondary antibody which is conjugated to either HRP or alkaline phosphatase is added and this is known as an indirect ELISA. The addition of a conjugated enzyme is used to measure the amount of solute which has been bound. A substrate is added after the conjugated antibody which results in the catalysation of the conjugated enzyme and the breakdown of the substrate into a coloured product which can be measured as optical density. The optical density gives the relative amount of coloured products allowing the measurement of the concentration or the titre of the test solutes. The HIV-1 gp140 ELISA which was used in this assay was based on the principle of the indirect ELISA whereby the antigen, which in this experiment was a gp140 trimer, was bound to the wells of a plate. Antibodies present in the sample were then able to bind to the antigen and these bound antibodies were detected with a secondary anti-monkey antibody conjugated with horseradish peroxidase. Horseradish peroxidase reacts with a chromogenic substrate which leads to a measurable colour change. The ELISA was used to

determine the titre of binding antibodies to the HIV-1 envelope in the plasma of the macaques used in this experiment.

Flat-bottomed 96-well Maxisorp^{TM} (Nunc) were coated with 10 ng/well of a soluble HIV-1 gp140 trimer (100) diluted in phosphate buffered saline (PBS) and incubated overnight at 4 °C. The wells were then washed once to remove unbound gp140 with 1X PBS using an automatic plate washer. Wells were then blocked for one hour with 5% skim milk (Sigma) in 1X PBS at room temperature and washed once with 1X PBS. Following the wash, the plasma samples were four-fold serially diluted from 1:20 in 2.5% skim milk in PBS and added to duplicate wells. A pooled sample, comprised of week 0 plasma from the macaques used in this study, was used as a negative control along with individual week 0 samples. Both the pooled week 0 samples and non-pooled week 0 samples were only diluted 1:20 and done in triplicate. Once all the required samples were loaded onto the plates, they were incubated overnight at 4°C. Following the overnight incubation, the plates were washed three times with PBST (PBS with 0.1% TWEEN 20) using an automatic plate washer. This was followed by adding 100 µL/well of anti-monkey IgG conjugated to horseradish peroxidase (HRP) (Merck) diluted 1:45 000 in PBS with 2.5% skim milk and left to incubate for one hour a room temperature. Plates were once again washed 3X with PBST using an automatic plate washer and this was followed by the addition of 100 µL/well of the substrate tetramethylbenzidine (TMB, Abcam). Plates were incubated for 10 minutes at room temperature before the reaction was stopped by adding 200 µL/well of 1N sulfuric acid (H_2SO_4). Optical density (OD) readings were measured on a VersaMax ELISA Microplate Reader (Molecular Devices Corporation) at 450nm and subtracted from the reference filter readings at 540nm to remove background. Cut-off OD values were determined by taking two times the mean OD of the pooled week 0 samples. Using these OD readings, the end-point titres were determined as the reciprocal of the highest dilution

that had a reading greater than the cut-off. The end-point titres were plotted against bleed time points using GraphPad Prism 5.0 software (weeks).

2.6 Single Genome Amplification (SGA)

SGA is based on a limiting dilution approach whereby the genetic material is diluted to the point where no more than 30% of successive PCR responses are positive. Under ideal circumstances, the mathematical probability that the amplicons produced later came from a single genome is greater than 80% (101). Limiting dilution was and continues to be a popular method for sequencing individual variants. To avoid PCR-induced recombination, a common occurrence when performing bulk sequencing, individually amplifying single variants is performed (102-104).

2.6.1 cDNA synthesis

Viral RNA was extracted as mentioned before using an ALLprep DNA/RNA kit (QIAGEN). This viral RNA was then used for cDNA synthesis. Two PCR mixes were prepared in the PCR clean room. The final concentrations of the reagents in the first premix were as follows: 1 µM Oligo(dT)20 (Invitrogen) and 0.4 µM dNTP mix (Life Technologies) per tube to make up 6 µL per tube of master-mix. The 6 µL of this master-mix was then aliquoted into 0.2 mL tubes to which 50 µL RNA was added later. The final concentrations of the reagents in the second PCR master-mix were as follows: 1X First-Strand Buffer (Invitrogen), + 5 mM DTT (Invitrogen), + 0.8 U/µL RNaseOUT (Invitrogen), + 10 U/µL SSIII RT (Invitrogen) and H_2O to a final volume of 44 µL. The SSIII RT, 5X First-Strand Buffer and DTT reagents are all part of the Superscript III Reverse Transcriptase kit (Invitrogen). The second premix was kept on ice while the thermo-cycler was heated to 65 °C. 50 µL of the extracted viral RNA was then added to the tube

containing 6 µL of the first PCR mix. This tube then contained 56 µL of RNA and PCR master-mix and was added to the thermo-cycler for the first cycle of disrupting the RNA secondary structure. The first cycle included a first step of heating at 65°C for five minutes followed by a second step of reducing the temperature to 4°C. While the thermocyclers temperature was at 4°C the 44 µL of the second PCR master-mix was added to the samples in the thermocycler. The first step of the second cycle started with an incubation at 50°C for one hour followed by another incubation step at 55°C for another hour. Once the incubation period was completed the SSIII RT was inactivated by heating the thermocycler to 70°C for fifteen minutes. The thermocycler was then cooled to 4°C at which stage 1 µL of RNase H was added and the samples were incubated for twenty minutes at 37°C to remove residual RNA from the cDNA molecule. Following this step, the cDNA was aliquoted and stored at -80°C.

2.6.2 Amplification & sequencing

To achieve less than 30% positive amplification reactions, cDNA was thawed and serially diluted to obtain the limiting dilution. A nested PCR was used for *env* amplification where two rounds of PCR produced the product, where the primers for the second round are nested within the first. Nine replicates for each dilution of sample were performed initially to determine the limiting dilution to use going forward. Each sample had a different limiting dilution to use as viral loads differed among monkeys as well as among samples and tissues used. 19 µL of the first round PCR mix consisting of 15.3 µL/reaction dH_2O, 1X High Fidelity Buffer, 2 mM magnesium sulfate ($MgSO_4$), 0.2 mM dNTPs, 0.025 U/µL Platinum® Taq DNA Polymerase High Fidelity enzyme, 0.2 µM Forward primer (DQ-SHIV50F) and 0.2 µM Reverse primer (DQ-SHIV51R) along with 1 µL of a cDNA sample was added to nine replicate wells of a 96 well plate for the first-round synthesis using the following forward and reverse primers: DQ SHIV50 (5’ – TAGAGCCCTGGAAGCATCCAGGAAGCAGGACTA - 3’) and DQ SHIV51

(5’ – TCCAGTCCCCCCTTTTCTTTTATAAAA – 3’). The samples were run on the thermocycler according to the parameters shown in Table 3:

Table 3. First round PCR cycling conditions for SGA.

Steps	**°C**	**Time**	**Cycles**
Initial denaturation	94	2 min	1 cycle
Denaturation	94	15 sec	35 cycles
Annealing	60	30 sec	
Extension	68	4 min*	
Final extension	68	10-20 min	1 cycle
Hold	4	∞	1 cycle
*The cycle is extended by an increment of 3 seconds each cycle.			

As with the first round PCR, the second master-mix consisted of 15.3 µL/reaction dH_2O, 1X High Fidelity Buffer, 2 mM magnesium sulfate ($MgSO_4$), 0.2 mM dNTPs, 0.025 U/µL Platinum® Taq DNA Polymerase High Fidelity enzyme, 0.2 µM Fwd primer (Env-C1) and 0.2 µM Rev primer (Env-C2) was added to 1 µL of the first round PCR sample to nine replicate wells in a PCR plate using the following forward and reverse primers: Env-C1 (5’ – ACCATGAGAGTGAAGGAGAAATAT – 3’) and Env-C2 (5’ – TCACAAGAGAGTGAGCTCGAGC – 3’). The samples were then run on the thermocycler according to the cycling conditions listed in Table 3.

The next step was to electrophorese the sample on an agarose gel. Four microlitres of the PCR sample was electrophoresed on a 1% agarose gel and stained with ethidium bromide (0.5

μg/mL). Positive wells were determined by the presence of a 2607 bp DNA fragment. If positivity was less than 30% for a sample the positive wells were purified using the MinElute PCR Purification Kit (QIAGEN) according to the manufacturer's instructions. The DNA concentrations of the resulting purified PCR products were then determined using a nanodrop (Nandrop^{TM} 1000 spectrophotometer). Sanger sequencing of the PCR products was done at the DNA Sequencing Unit at Stellenbosch University using twelve gp160 primers which spanned the entire length of *env* (Appendix D). Sequences were analysed using CLC Main Workbench 8.

Results

3.1 Viral RNA loads in PBMCs and lymphoid tissue of macaques 18-21 weeks after SHIVC109P7 intra-rectal challenge.

RNA was extracted from PBMCs, splenocytes and inguinal and mesenteric lymph nodes of control and vaccine group macaques at 18-21 weeks after the first intra-rectal challenge and used to determine RNA viral loads of SHIVC109P7.

Four of the five animals (P4, P11, P25 & P52) in the vaccine group had detectable viral loads in their PBMCs in contrast to the control group in which only P67 had a detectable viral load (Figure 3.1). For the vaccine group, the median viral load in the PBMCs (Figure 3.2) was 12.5712 *gag* copies/10^7 cells; (range: 0.1387 *gag* copies/10^7 cells – 61.1528 *gag* copies/10^7 cells). For the control group, the median viral load in the PBMCs (Figure 3.2) was 0.4274 *gag* copies/10^7cells; (range: 0.0993 *gag* copies/10^7 cells – 19.717 *gag* copies/10^7 cells). P4 and P67 had the highest viral load copies in vaccine and control groups respectively. Of the animals in the control group only P67 had a viral load greater than one whereas in the vaccine group only P47 had a viral load lower than one. The median of the averages of the viral loads for PBMCs was 3.82 copies/10^7 cells with a range of <1 copies/10^7 cells to 61.15 copies/10^7 cells.

All animals except P47 had detectable viral loads in the mesenteric tissues (Figure 3.1). For the vaccine group, the median viral load in the mesenteric tissues (Figure 3.2) was 42.3658 *gag* copies/10^7 cells; (range: 12.7127 *gag* copies/10^7 cells – 92.5242 *gag* copies/10^7 cells). For the control group, the median viral load in the mesenteric tissues (Figure 3.2) was 48.0127 *gag* copies/10^7 cells; (range: 18.2018 *gag* copies/10^7 cells – 376.6517 *gag* copies/10^7 cells). P52 had the highest viral load (92.5 *gag* copies/10^7 cells) of the vaccine group animals and P72 had the highest mean viral load (376.6 *gag* copies/10^7 cells) of the control group animals. Overall P70 and P71 (23.9 and 18.2 *gag* copies/10^7 cells) had lower viral loads than three of the five vaccine group animals with only P72 having a viral load greater than P52. The median of the averages of the viral loads for the mesenteric tissues was 42,37 copies/10^7 cells with a range of 12.71 copies/10^7 cells to 376.65 copies/10^7 cells.

All animals had detectable viral loads in the inguinal tissues (Figure 3.1). For the vaccine group, the median viral load in the inguinal tissues (Figure 3.2) was 58.08 *gag* copies/10^7 cells; (range: 8.85 *gag* copies/10^7 cells – 70.69 *gag* copies/10^7 cells). For the control group, the median viral load in the inguinal tissues (Figure 3.2) was 76.335 *gag* copies/10^7 cells; (range: 22.36 *gag* copies/10^7 cells – 911.61 *gag* copies/10^7 cells). P25 and P52 had the highest detectable viral loads for the vaccine group animals at 70.69 and 70.67 gag copies/10^7 cells, respectively. The viral load in the inguinal tissue of P47 were very low at 8.85 *gag* copies/10^7 cells. The control group animal P71, had the highest viral load of 911.61 *gag* copies/10^7 cells. The median of the averages for the RNA viral loads in the inguinal tissue cells was 58.08 copies/10^7 cells with a range of 8.85 copies/10^7 cells to 911.61 copies/10^7 cells.

All animals had detectable viral loads for the splenocytes (Figure 3.1). For the vaccine group, the median viral load in the splenocytes (Figure 3.2) was 12.3902 *gag* copies/10^7 cells; (range: 7.6776 *gag* copies/10^7 cells – 648.7835 *gag* copies/10^7 cells). For the control group, the median viral load in the splenocytes (Figure 3.2) was 633.188 *gag* copies/10^7 cells; (range: 9.1945 *gag* copies/10^7 cells – 5283.254 *gag* copies/10^7 cells). P4 had the highest viral load for the vaccine group at 648.7 *gag* copies/10^7 cells while P11 had the lowest viral load across both groups of animals with 7.6 *gag* copies/10^7 cells. P71 had the highest viral loads in the control group as well as overall with 5283.25 *gag* copies/10^7 cells. P72 had the lowest viral load for the control group with a viral load of 9.19 *gag* copies/10^7cells. There was a high variability in the viral loads in the splenocytes between the different animals. The variability could be seen between animals in the vaccine and control groups as well as across both groups. The median of the averages for the RNA viral loads in the splenocytes was 26,13 copies/10^7 cells with a range of 7.77 copies/10^7 cells to 5283.25 copies/10^7 cells.

There was no significant difference between the two groups within tissues where significance was determined by a P-value less than 0.05 (Figure 3.2). The P-values for the independent t-test conducted on the PBMC between the control and vaccine groups gave a P-value of 0.3604. P-values for mesenteric: 0.4230, inguinal: 0.2781, and splenocytes: 0.1158 are all greater than the significance cut-off meaning there is no significant difference between the viral loads observed for the control and vaccinated macaques. There was also no significance (P= 0.3104) in RNA viral loads between PBMC and lymphoid tissues (Figure 3.2).

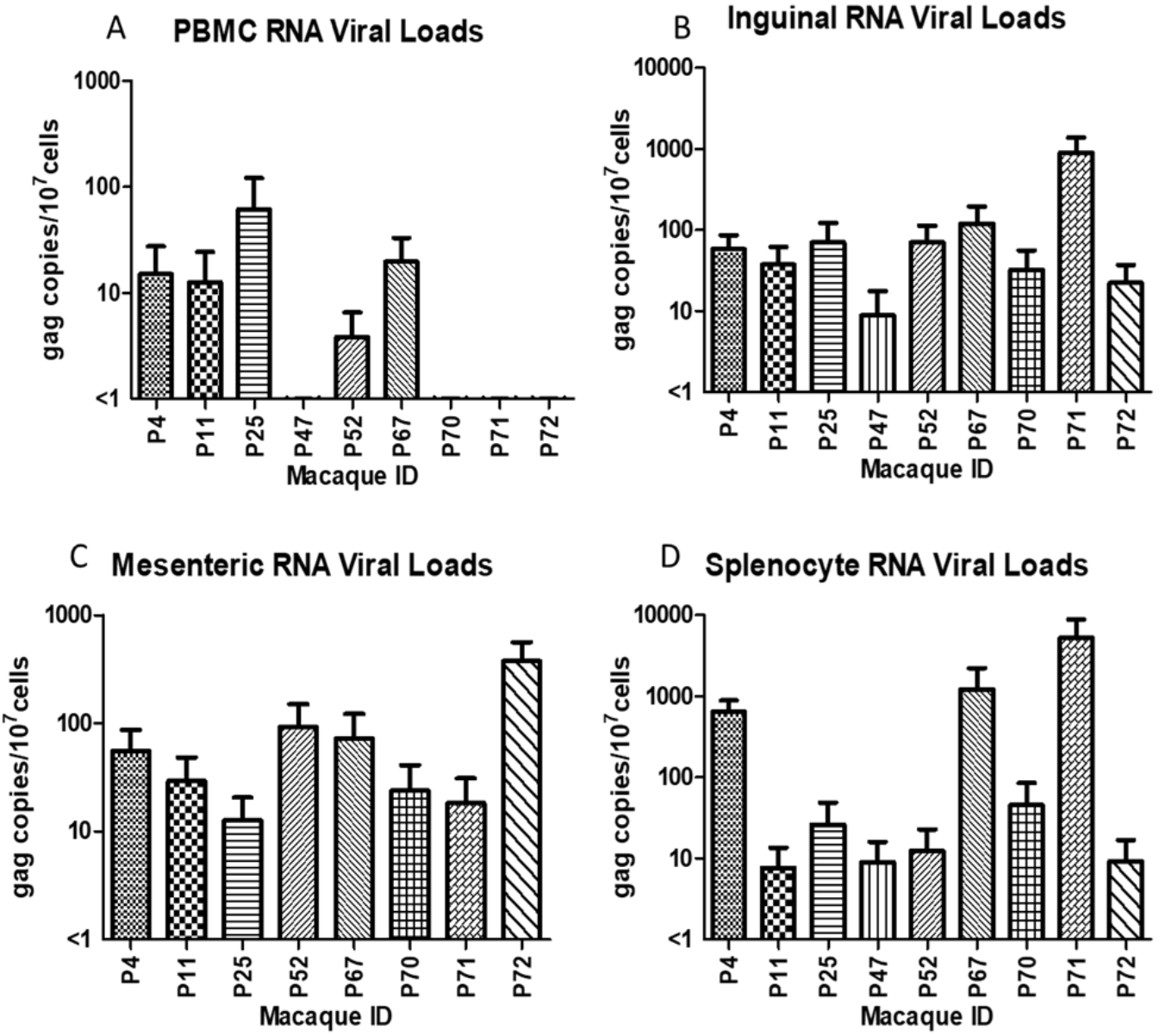

Figure 3. 1: RNA viral loads in PBMCs and lymphoid tissue of macaques 21 weeks after initiation of challenges. The graphs A-D compare the viral loads obtained from the vaccine group (P4, P11, P25, P47, and P52) and the control group (P67, P70, P71, and P72) animals in the different tissues. The bars represent the average quantity of *gag* copies per 10^7 cells with the standard error of the mean (SEM) shown. Mean and SEM of the RNA viral loads were determined by repeating the experiment three times in triplicate.

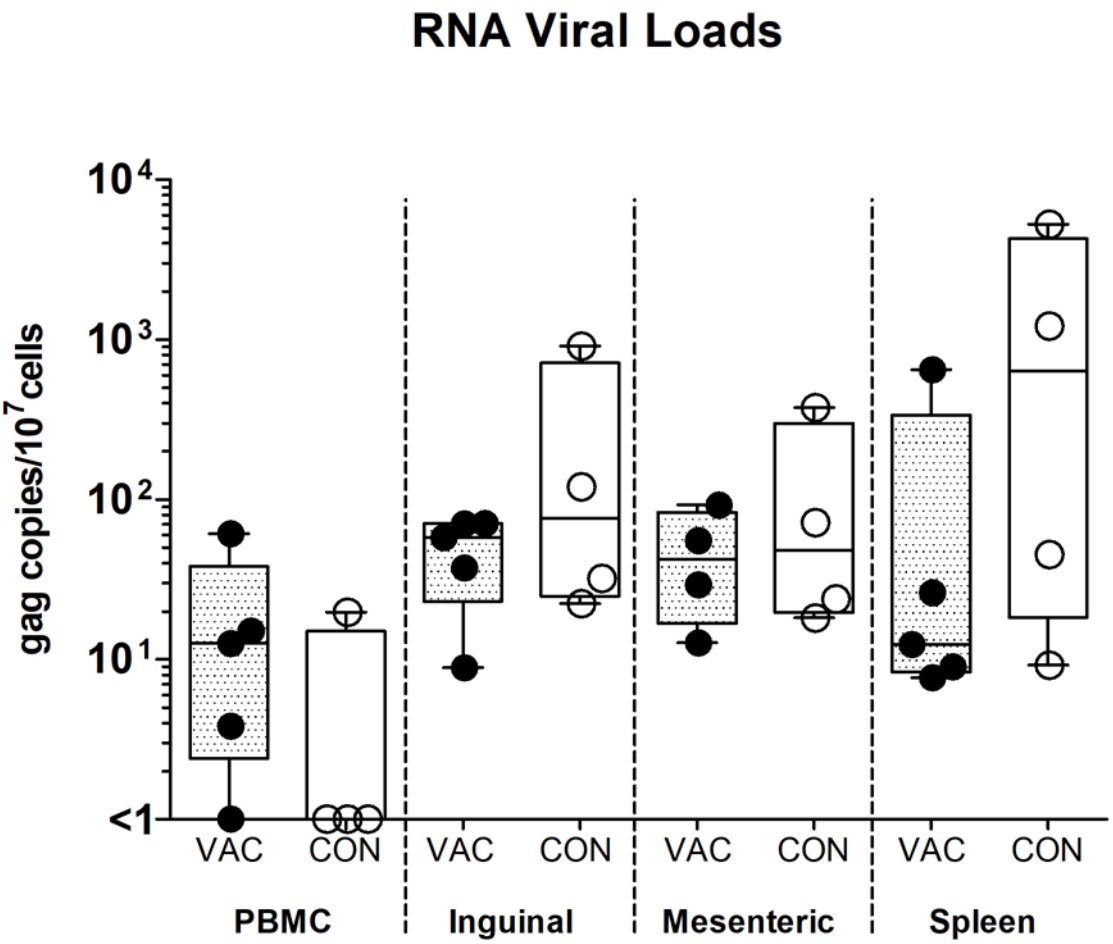

Figure 3. 2: Comparison of RNA viral loads in vaccinated and control group macaques. Graph showing the range, and median viral loads of vaccinated (VAC; solid circle & dotted boxes) and unvaccinated (CON; open circles & clear boxes) animals. The medians are indicated with horizontal bars across the boxes. Significance was calculated using the Mann-Whitney t-test, two-tailed with the significance cut-off at P= 0.05. There was no statistical significance between RNA viral loads of the vaccinated and control groups for either the lymphoid tissues or the PBMCs. P-values for the PBMC, inguinal, mesenteric, and spleen are as follows; PBMC = 0.3061, inguinal = 0.7302, mesenteric = 0.8857, and spleen = 0.1905 (P-values not shown on the graph).

3.2 Proviral DNA loads in PBMCs and lymphoid tissue of macaques 21 weeks after initiation of intra-rectal SHIVC109P7 challenges.

DNA was extracted from PBMCs, splenocytes and cells isolated from inguinal and mesenteric lymph nodes to comparatively analyse the amount of integrated provirus in peripheral blood and lymphoid tissues. All animals had detectable PBMC proviral DNA levels (Figure 3.3). For the vaccine group, the median proviral DNA load in the PBMCs (Figure 3.4) was 1930.854 *gag* copies/10^7 cells; (range: 1079.886 *gag* copies/10^7 cells – 28 663,.88 *gag* copies/10^7 cells). For the control group, the median proviral DNA load in the PBMCs (Figure 3.4) was 1405,058 *gag* copies/10^7cells; (range: 696.925 *gag* copies/10^7 cells – 2415.786 *gag* copies/10^7 cells). P4 and P70 had the highest levels for animals in the vaccine and control groups respectively with values of 28 663.9 and 2415.786 *gag* copies/10^7 cells. The lowest PBMC proviral DNA amount for the vaccine group was that observed for P52 with a value of 1079.89 *gag* copies/10^7cells. P71 had the lowest value overall with a proviral DNA level of 696.93 *gag* copies/10^7 cells. The median of the averages for proviral DNA loads for PBMCs was 1903.98 copies/10^7 cells with a range of 696.93 copies/10^7 cells to 28 663.88 copies/10^7 cells.

All four vaccine group animals, that mesenteric tissue was obtained from, had detectable proviral DNA (Figure 3.3). As mentioned earlier, no mesenteric tissue was obtained from macaque P47 of the vaccine group. For the vaccine group, the median proviral DNA load in the mesenteric tissues (Figure 3.4) was 3296.323 *gag* copies/10^7 cells; (range: 1133.575 *gag* copies/10^7 cells – 3 198 678 *gag* copies/10^7 cells). For the control group, the median proviral DNA load in the mesenteric tissues (Figure 3.4) was 5294.07 *gag* copies/10^7cells; (range: 3744.342 *gag* copies/10^7 cells – 26831.68 *gag* copies/10^7 cells). P52 had the highest overall

amount of mesenteric proviral DNA with a value of 3 198 678 *gag* copies/10^7 cells. P70 had the highest mesenteric proviral DNA value for the control group with 26831.7 *gag* copies/10^7 cells. P25 (vaccine group) and P67 (control group) had the lowest mesenteric proviral DNA values with 1133.57 and 3744.34 *gag* copies/10^7 cells, respectively. The median of the averages for proviral DNA loads for mesenteric tissues was 4304,11 copies/10^7 cells with a range of 1133.58 copies/10^7 cells to 3 198 678 copies/10^7 cells.

All animals had detectable proviral DNA loads in the inguinal tissues (Figure 3.3). For the vaccine group, the median viral load in the inguinal tissues (Figure 3.4) was 3160.362 *gag* copies/10^7 cells; (range: 1024.548 *gag* copies/10^7 cells – 17 411.43 *gag* copies/10^7 cells). For the control group, the median viral load in the inguinal tissues (Figure 3.4) was 19 030.61 *gag* copies/10^7 cells; (range: 604.469 *gag* copies/10^7 cells – 73 140.68 *gag* copies/10^7 cells). P25 and P70 had the highest detectable viral loads for the vaccine group and control group animals respectively at 17 411.43 *gag* copies/10^7 cells and 73 140.68 *gag* copies/10^7 cells. P72 had the lowest inguinal proviral DNA value overall with 604.46 *gag* copies/10^7 cells and P52 had the lowest proviral DNA value for the vaccine group with 1024.55 *gag* copies/10^7 cells. The median of the averages for proviral DNA loads in the inguinal tissue cells was 3160.36 copies/10^7 cells with a range of 604.67 copies/10^7 cells to 73 140.68 copies/10^7 cells.

All animals had detectable proviral DNA levels in the splenocytes (Figure 3.3). For the vaccine group, the median viral load in the splenocytes (Figure 3.4) was 1827.661 *gag* copies/10^7 cells; (range: 238.1755 *gag* copies/10^7 cells – 53 156.65 *gag* copies/10^7 cells). For the control group, the median viral load in the splenocytes (Figure 3.4) was 2417.451 *gag* copies/10^7 cells; (range: 1353.013 *gag* copies/10^7 cells – 3250.949 *gag* copies/10^7 cells). P25 had the largest amount of splenocyte proviral DNA with a value of 53 156.7 *gag* copies/10^7cells, P11 had the second largest amount for the vaccine group with 2573.65 *gag* copies/10^7 cells. For the control group P67 had the largest value for splenocyte proviral DNA 3250.95 *gag* copies/10^7 cells with P72 having the second largest amount with 3025.23 *gag* copies/10^7 cells. P47 had the lowest total for the vaccine group with an overall value of 238.176 *gag* copies/10^7 cells. P71 had the lowest splenocyte proviral DNA value in the control group with 1353.01 *gag* copies/10^7 cells. The median of the averages for proviral DNA loads for splenocytes was 1827,66 copies/10^7 cells with a range of 238.18 copies/10^7 cells to 53 156.65 copies/10^7 cells.

Significance was determined between the vaccine and control groups within tissues by using the independent t-test. There was no significant difference between the two groups within tissues where significance was determined by a P-value less than 0.05 (Figure 3.4). The P-values for the independent t-test conducted on the PBMC between the control and vaccine groups gave a P-value of 0.2857. P-values for mesenteric: 0.6857, inguinal: 1.0000, and splenocytes: 0.9048 are all greater than the significance cut-off meaning there is no significant difference between the proviral DNA loads present in the control and vaccinated macaques (Figure 3.4).

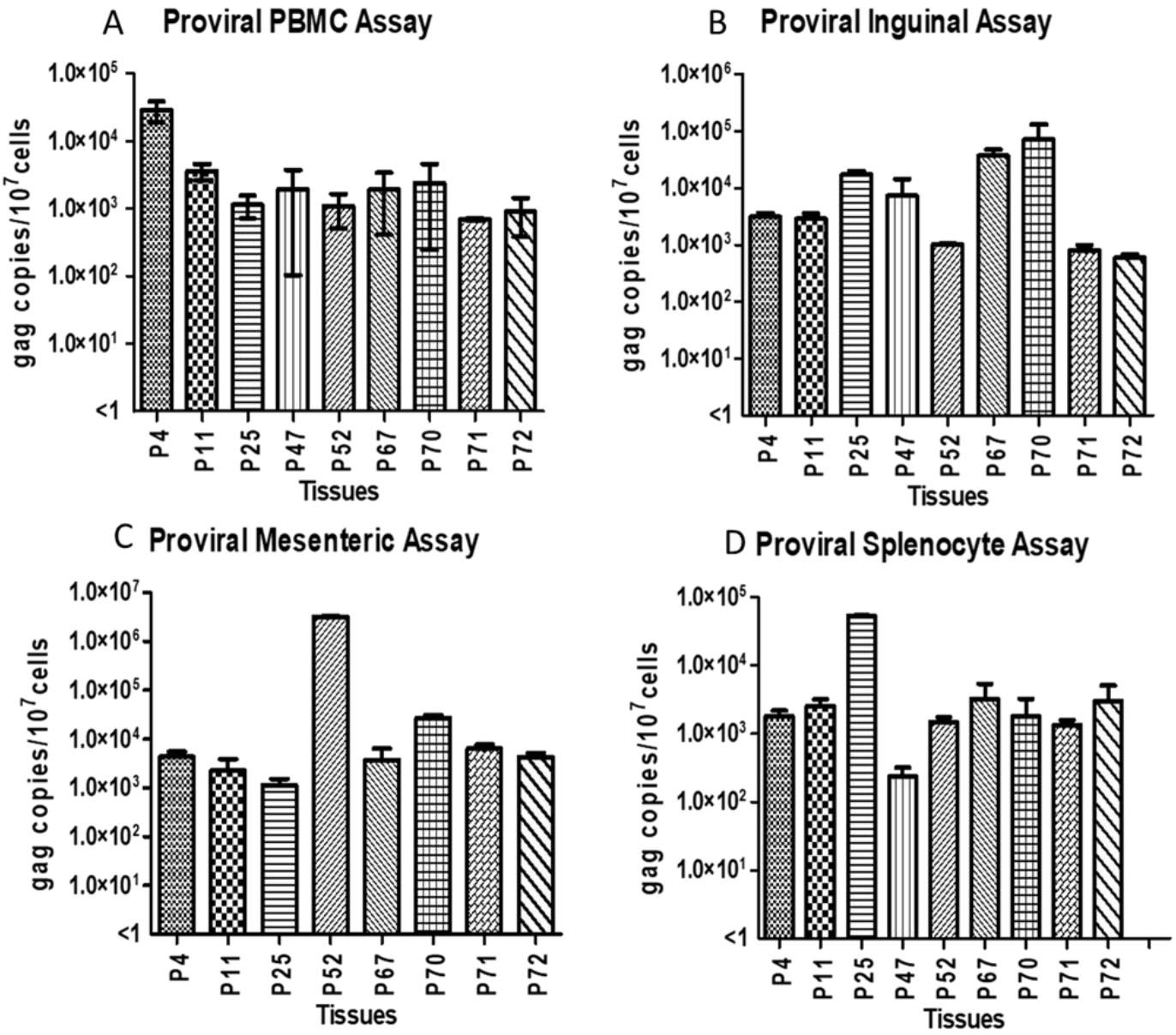

Figure 3. 3: Proviral DNA loads in PBMCs and lymphoid tissue of macaques 21 weeks after initiation of challenges. Graphs A-D compare the proviral DNA loads for the vaccine group (P4, P11, P25, P47, and P52) and the control groups (P67, P70, P71, and P72) animals in the different tissues. The bars represent the average quantity of *gag* copies per 10^7 cells with the standard error of the mean (SEM) shown. Mean and SEM of the Proviral DNA loads were determined by repeating the experiment three times in triplicate.

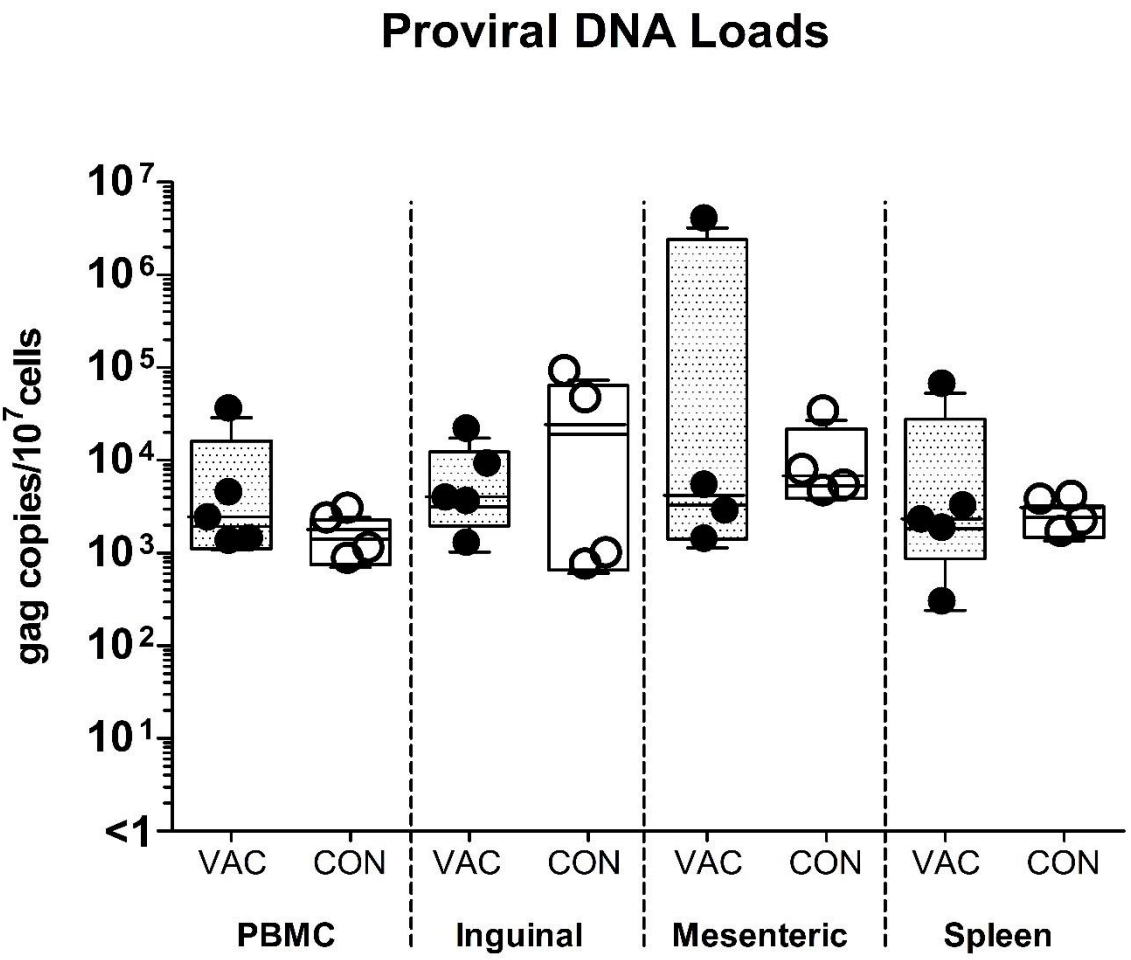

Figure 3. 4: Comparison of Proviral DNA loads in vaccinated and control group macaques. Graph showing the range, and median viral loads of vaccinated (VAC; solid circle & dotted boxes) and unvaccinated (CON; open circles & clear boxes) animals. The medians are indicated with horizontal bars across the boxes. Significance was calculated using the Mann-Whitney t-test, two-tailed with the significance cut-off at P= 0.05. There was no statistical significance between Proviral DNA loads of the vaccinated and control groups for either the lymphoid tissues or the PBMCs. P-values for the PBMC, inguinal, mesenteric, and spleen are as follows; PBMC P= 0.2857, inguinal P= 1.0000 mesenteric= 0.6857, and spleen= 0.9048 (P values not shown on graph).

3.3 Western Blot Results

An in-house Western blot procedure was used to simultaneously detect Env and Gag-specific binding antibodies in macaque plasma at different time points. The process of developing this western blotting assay began by confirming the rMVA expression of *gag* and *env* by immunofluorescence (Figure 3.5 A). Following confirmation by immunofluorescence Env and Gag were detected on a blot using commercial antibodies and examining the banding patterns

(Figure 3.5 B -C). Once it was determined that Gag and Env were present in rMVA with commercial antibodies, different plasma dilutions were run to determine the optimal dilution to use going forward. The dilution used was determined by looking at the banding patterns of the different dilutions and using the dilution that had the lowest background with the strongest Gag and Env bands present.

The Western blots in Figure 3.5 were probed with a 1:200 dilution of macaque plasma. Bands were seen at approximately 150 kDa (HIV-1 Env) and 55 kDa (SIV Gag) with plasma obtained at weeks 13, 32 and 53 for all vaccine group animals, indicating that binding antibodies to HIV-1 Env and SIV Gag were present. The intensity of the bands varied from animal to animal. Plasma isolated at week 13 for the vaccine group corresponds to the time point one week after the final MVA inoculation. Plasma obtained at week 32 corresponds to the time point immediately prior to SHIV challenge and 4 weeks after the final protein inoculation and week 53 was when the macaques were sacrificed. Plasma obtained from the control group macaques prior to challenge (week 0) and at sacrifice (week 53) was used. Despite bands for the antigens being noticeable, a large amount of non-specific reactivity was also present. Multiple bands were seen for the week 0 time points, indicating that there were antibodies present in the plasma that bound to antigens in the cell lysates other than HIV-1 Env and SIV Gag, as macaques had not been vaccinated or challenged at this time point.

Macaque P38 was used as the control in this experiment as it was excluded from data analyses because it was not euthanized at the same time as the other macaques in this project. Even though it was excluded from the experimental groups it was determined that the samples could be used as controls for optimizing experiments.

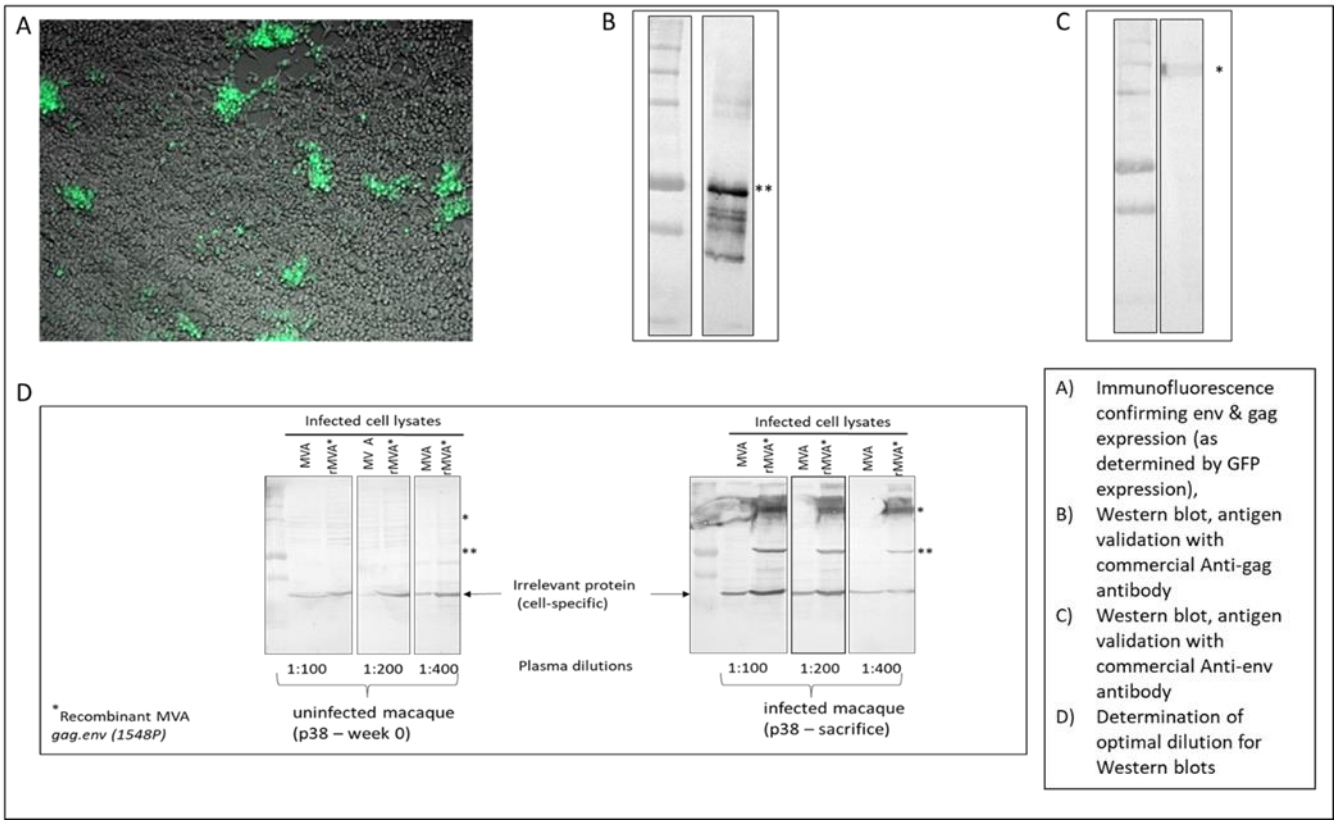

Figure 3. 5: Development of the Western blotting assay. The process of development for the Western blotting assay beginning with the confirmation of env and gag expression (A) by GFP immunofluorescence. Gag and Env antibody validation were performed with commercial anti-Env/Gag antibodies (B, C) and finally the optimal dilution for the western blots were obtained using macaque P38 (D).

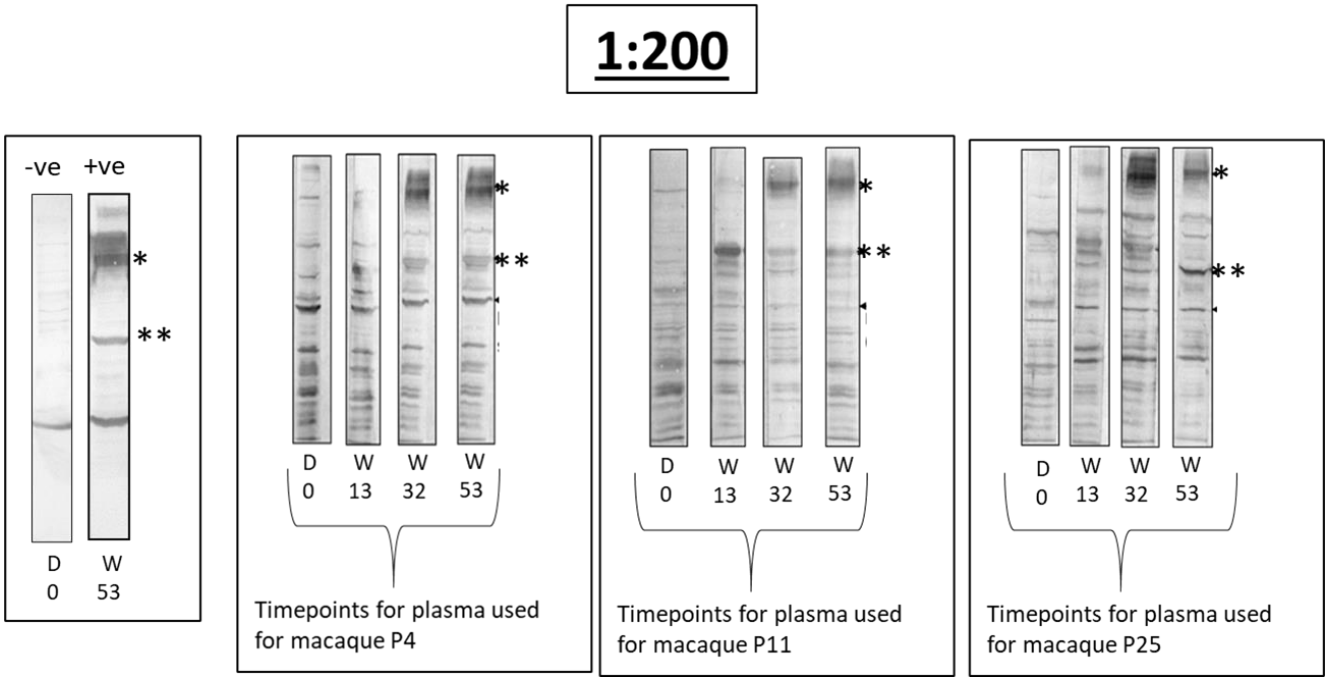

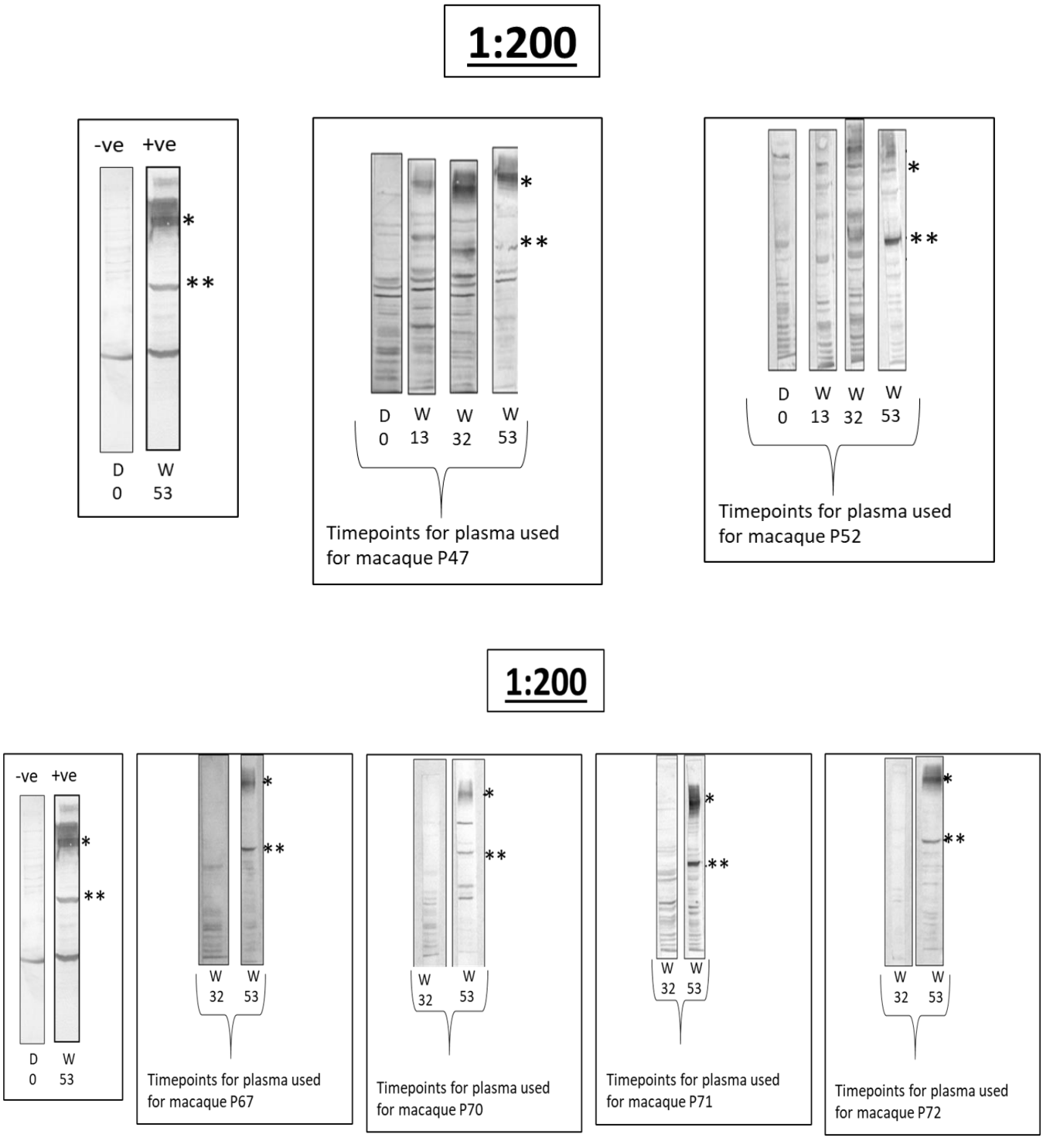

Figure 3. 6: Western Blots for macaques P4 to P72 showing binding antibodies to HIV-1 Env and SIV Gag. A 1:200 dilution of the plasma used. The time points at which the plasma was isolated are indicated below each strip. 0 = prior to vaccination and weeks 13, 32 and 53. * = HIV Env. ** = SIV Gag. -ve = negative control taken from the plasma of macaque P38 prior to vaccination. +ve = positive control taken from macaque P38 at week 53.

Despite bands for the HIV-1 Env and SIV Gag antigens being noticeable, indicating the presence of binding antibodies to these antigens, a large amount of non-specific reactivity was also present. To reduce non-specific reactivity the macaque plasma was preabsorbed with cell lysate from HEK293T cells infected with wild type MVA. Different dilutions were used to determine the optimal dilution where signals to non-specific antigens were lowest and binding to HIV-1 Env and SIV Gag was still distinctly visible. Despite preabsorbing and diluting the macaque plasma, binding of antibodies to non-specific antigens were still detected at all timepoints (Figure 3.6).

Binding antibodies to SIV Gag and HIV Env were present in all the tested plasma samples. However, these results were not quantifiable and therefore a binding antibody ELISA was performed to quantify the levels of binding antibodies to HIV Env.

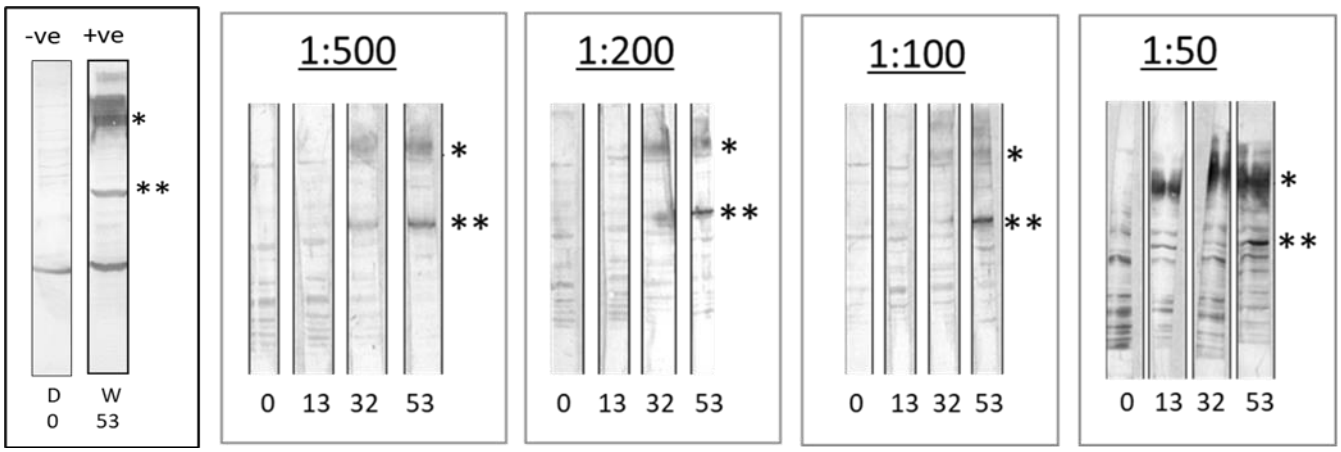

Figure 3. 7: Optimisation of a Western blotting assay: to confirm the presence of antibodies to HIV-1 Env and SIV Gag in the plasma of macaque P4. Different dilutions of the preabsorbed plasma used 1:500 to 1:50 are shown. The time points at which the plasma was isolated are indicated below each strip. 0 = prior to vaccination and weeks 13, 32 and 53. * = HIV Env. ** = SIV Gag. -ve = negative control taken from the plasma of macaque P38 prior to vaccination. +ve = positive control taken from macaque P38 at week 53.

3.4 ELISA

3.4.1 Levels of binding Env-gp140 antibody responses in macaque plasma.

An ELISA method was used to measure the Env IgG antibodies in the macaque blood. The endpoint titres and cut-off points for the ELISA were determined and are mentioned in the corresponding methods section. Prior to running the full experiment plasma from macaque P38 was used for optimization. Optimization involved determining the correct dilution to use for both the secondary antibody as well as determining the optimal range of serial dilutions of the plasma to use. Three dilutions for the secondary antibody were tested, 1:45 000, 1:30 000 and 1:10 000. Figure 3.7 shows the graph produced after the initial optimization experiment. It was determined that the 1:45 000 dilution of the secondary antibody was optimal as this dilution gave a low signal at week 0 but still gave a strong signal at week 22. During the optimization it was also determined that a 4-fold serial dilution starting with a 1:20 dilution was an optimal dilution series for the macaque plasma being used. Serial dilutions of macaque plasma were made and plotted against the OD reading obtained (Figure 3.8). Binding antibody endpoint titres were determined as the reciprocal of the highest dilution that had a reading greater than the cut-off.

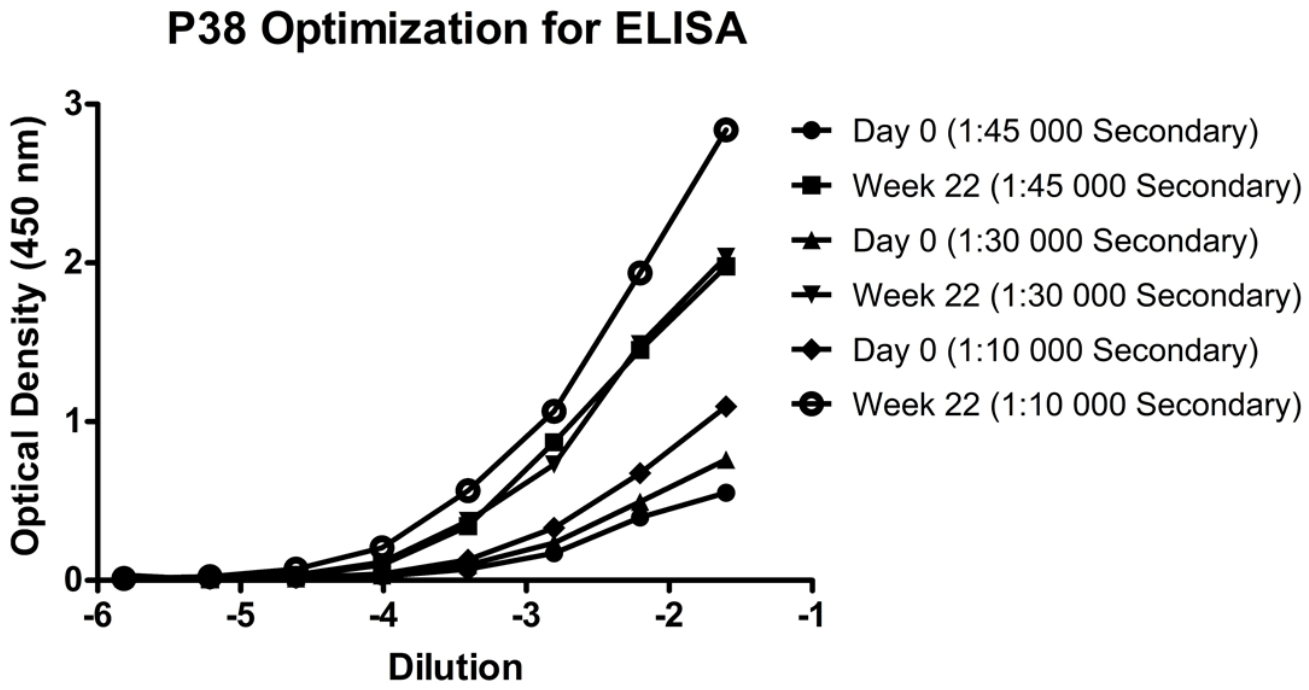

Figure 3. 8: ELISA optimization using macaque P38: This graph was used to determine the optimal dilution for the secondary antibody. The optimal dilution would be the dilution at which there was a weak signal for day 0 but a strong signal at week 22.

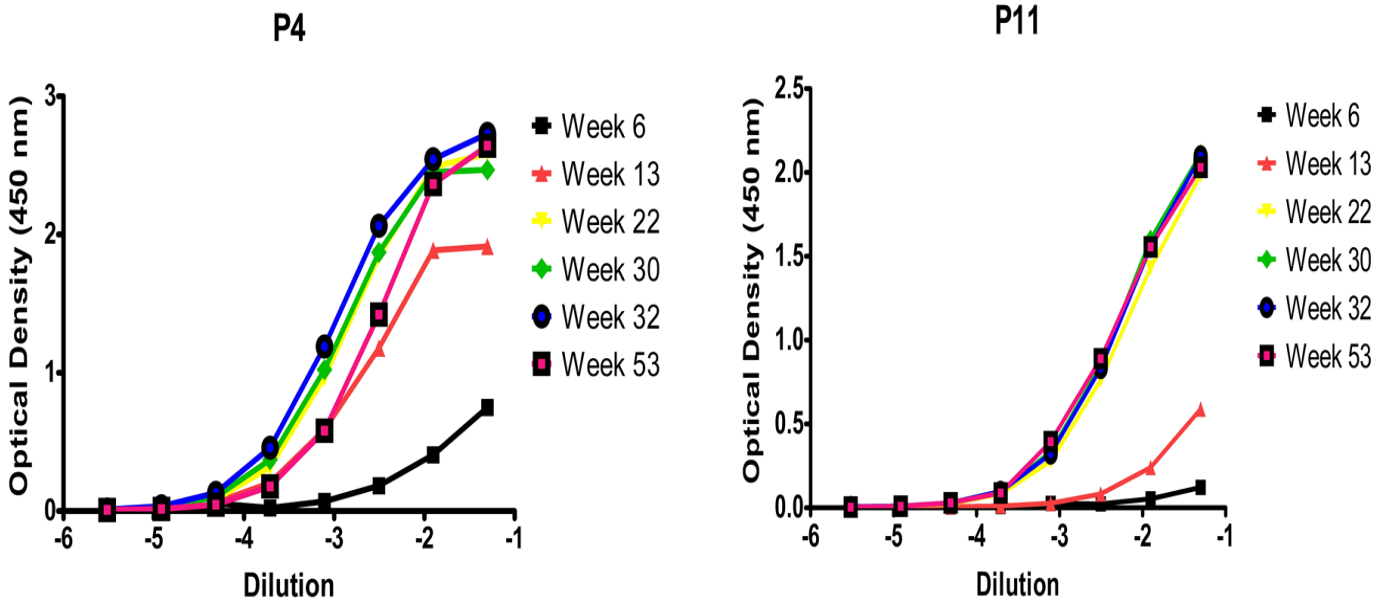

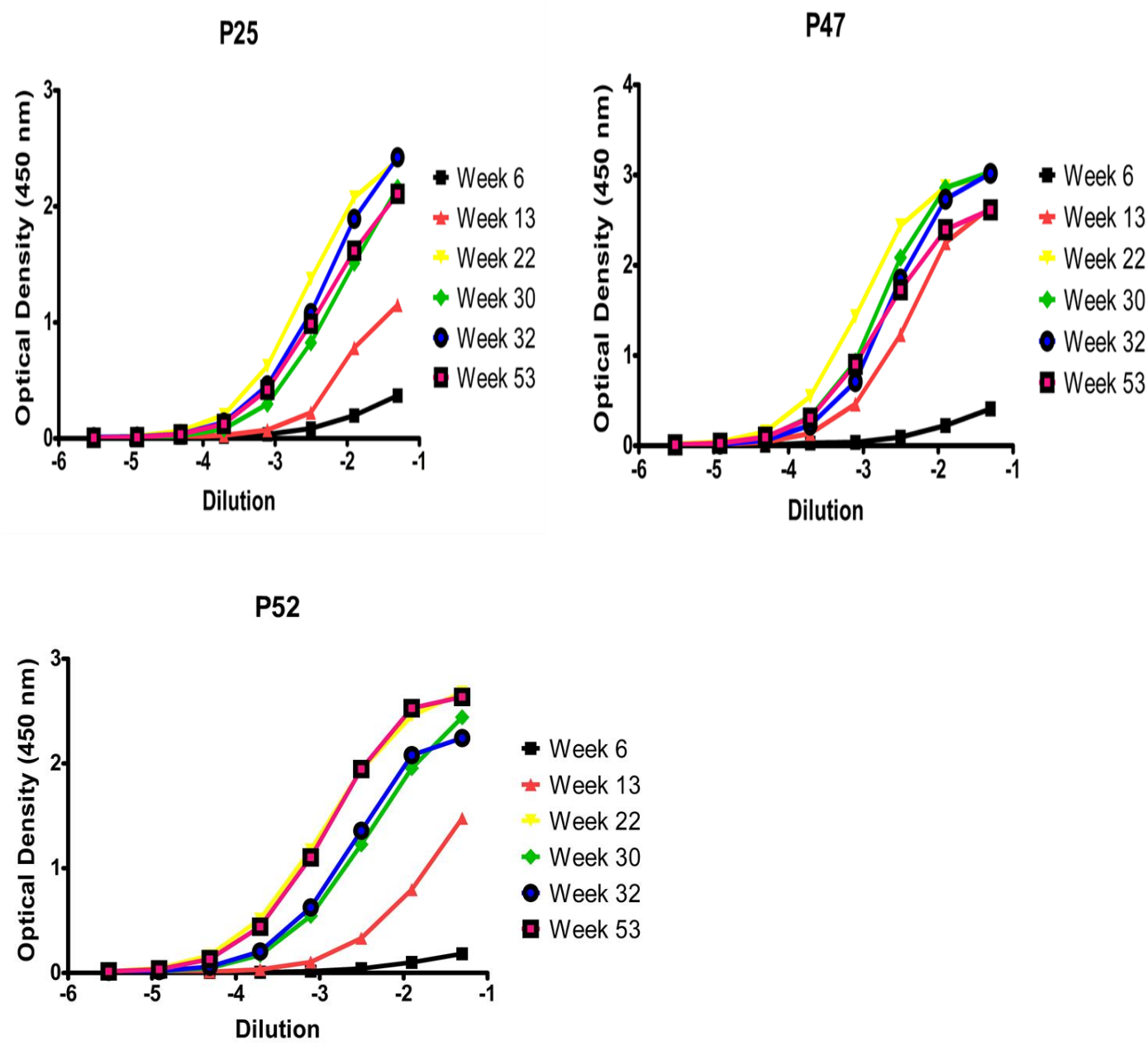

Figure 3. 9: Graphs showing the change in optical density with serial dilution of plasma from vaccinated macaques at different time points: Serial dilutions of macaque plasma were made and plotted against the OD reading obtained.

Endpoint titres for the macaques are presented in Figure 3.10. At week 6 (median endpoint titre: 80, range: 0-80) two weeks after the second DNA vaccination, antibodies were detected in macaques P4, and P11. No antibodies were detected for macaques P25, P47, and P52 at this time point. Binding antibodies titres saw a steep rise between weeks 6, two weeks after 2nd

DNA vaccination, and 13 (median endpoint titre: 680, range: 20- 1280) one week after the 2nd MVA vaccination for macaques P4, P25, P47, and P52. While antibodies were detected at week 6 for macaque P11 antibody titres decreased to undetectable levels at week 13. Between week 13 (one week after 2nd MVA) and week 22 (median endpoint titre: 5120, range: 320- 5120) two weeks after the first protein boost there was a steep rise in antibody titres for all vaccinated macaques. Between weeks 22 (two weeks after first protein boost) and 30 (median endpoint titre: 1280, range: 320- 5120) two weeks after second protein boost there was a decrease in binding antibody titres of macaques P25, P47 and P52. For macaque P4 the antibody titre plateaued between these timepoints, P11 however saw an increase in binding antibody titres during this same period. Between week 30 and week 32 (median endpoint titre: 1280, range: 1280- 5120) the day of the first challenge, macaques P4, P11, P47 and P52 had no change in the binding antibody titre whereas macaque P25 had an increase in the binding antibody titre. The binding antibody titres between week 32, day of the first challenge, and week 53 (median endpoint titre: 1280, range: 1280- 5120) the day of euthanasia, remained the same for macaques P11, P25, and P47 meaning the titres had plateaued. Macaque P4 had a decrease in binding antibody titres between week 32 and 53 while macaque P52 saw an increase in the binding antibody titre. Macaques P4 (5120), P25 (1280), P47 (5120), and P52 (5120) had peak endpoint titres at week 22 while macaque P11 reached its peak endpoint titre (1280) at week 30.

In Figure 3.10 the endpoint titres for the control animals are plotted against the vaccine group animals. All control animals had undetectable endpoint titres at week 32 (prior to viral challenge) and at week 53 (median endpoint titre: 3200, range: 1280- 20 480) after they had been challenged all the macaques in the control group had detectable endpoint titres. P71 had the highest antibody titre out of the control animals while P67 and P70 had the lowest.

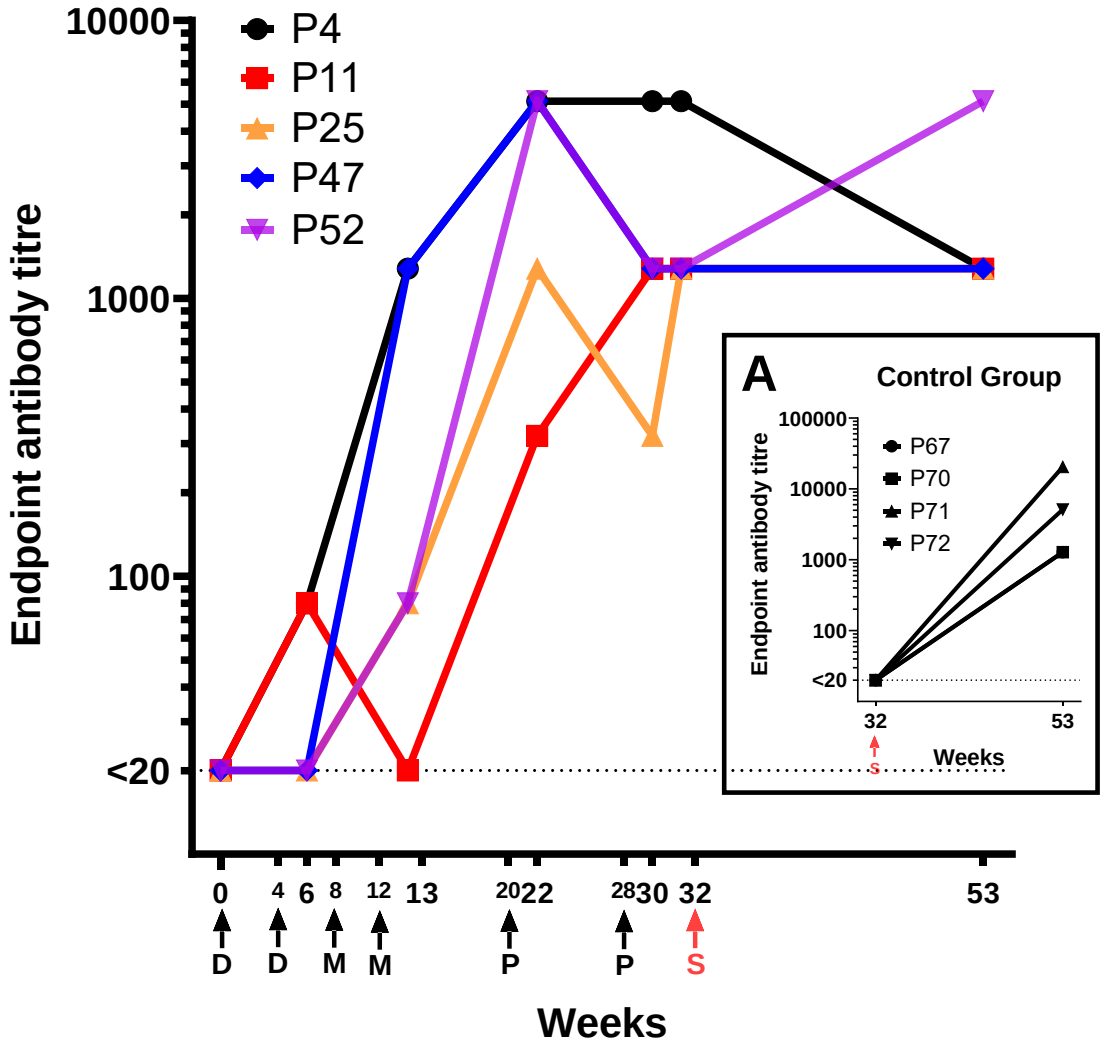

Figure 3. 10: Endpoint gp140 Env antibody titres to HIV Env for vaccinated macaques 18-21 weeks after the first challenge. Gp140 Env-specific antibodies in the plasma obtained from vaccinated macaques at baseline (week 0) and selected time points post DNA (week 6), MVA (week 13) and gp140 Env protein (weeks 22, 30, 32) vaccinations and post SHIV challenge (week 53) were measured using a standard ELISA method. Antibody titres of <20 (dotted line) were considered negative. Vaccination time points and when intrarectal SHIV challenges were initiated are indicated by arrows (D= DNA; M= MVA; P=gp140 Env protein; S=SHIV). (A) (inset) Represents the endpoint antibody titres in the control animals at pre- (week 32) and post- (week 53) intrarectal SHIV challenge.

3.5 Sequencing of the envelope gene from SHIV isolated from different sites in the macaques.

Sequencing of the envelope gene was performed to determine whether SHIV sequences varied between PBMCs and various lymphoid tissue sites for control and vaccinated macaques. PBMC viral RNA levels were extremely low for both control and vaccine animals therefore sequences for only three animals were obtained from PBMCs. The other site that was looked at for this project was the inguinal lymph node tissue. Sequences for 6 animals' inguinal lymph nodes were obtained for P4, P11, P25, P52, P70 and P72 (Figure 3.11). There were minimal differences between all sequences apart from two sequences from the PBMC of macaque P67 which did not have a stop codon in the correct position (Figure 3.11 C). Apart from these two sequences there was a 98-99% similarity between the remaining sequences at the amino acid level, with the most differences between two sequences being 16 amino acids (Figure 3.11). Figure 3.11 D shows the comparison between the sequences obtained from the inguinal tissues of P25 and P70. These two animals were chosen as they had the most sequences to analyze. The obtained sequences also had very few differences to the SHIV virus that the macaques had been challenged with. There were amino acid differences at potential N-glycosylation sites (PNGS) in the variable region 1 (V1), glycan N276 in the conserved region 2 (C2) and variable region 4 (V4) (Figure 3.12 & 3.13). The amino acid changes present at the V1 and V2 sites led to the PNGS shifting. Amino acid changes in the C2 region resulted in additional PNGS being created.

A: Vaccine group animals

		1	2	3	4	5	6	7	8	9	10	11	12	13	14	15	16	17
P4i1	1		0	3	5	5	8	8	7	11	11	11	9	5	5	4	6	7
P4i2	2	100,00		3	5	5	8	8	7	11	11	11	9	5	5	4	6	7
P4i3	3	99,65	99,65		2	2	5	5	4	8	8	8	6	2	2	1	3	4
P11i1	4	99,42	99,42	99,77		2	7	7	6	10	10	10	8	4	4	1	3	6
P11i2	5	99,42	99,42	99,77	99,77		7	7	6	10	10	10	8	4	4	1	3	6
P25i1	6	99,07	99,07	99,42	99,19	99,19		0	1	7	7	9	7	7	7	6	8	3
P25i2	7	99,07	99,07	99,42	99,19	99,19	100,00		1	7	7	9	7	7	7	6	8	3
P25i3	8	99,19	99,19	99,53	99,30	99,30	99,88	99,88		8	8	8	6	6	6	5	7	2
P25i4	9	98,72	98,72	99,07	98,84	98,84	99,19	99,19	99,07		6	16	14	10	10	9	11	10
P25i5	10	98,72	98,72	99,07	98,84	98,84	99,19	99,19	99,07	99,30		14	14	10	10	9	11	10
P52i2	11	98,72	98,72	99,07	98,84	98,84	98,95	98,95	99,07	98,14	98,37		2	10	10	9	11	8
P52i3	12	98,95	98,95	99,30	99,07	99,07	99,19	99,19	99,30	98,37	98,37	99,77		8	8	7	9	6
P4P1	13	99,42	99,42	99,77	99,53	99,53	99,19	99,19	99,30	98,84	98,84	98,84	99,07		0	3	5	6
P4P2	14	99,42	99,42	99,77	99,53	99,53	99,19	99,19	99,30	98,84	98,84	98,84	99,07	100,00		3	5	6
P11P1	15	99,53	99,53	99,88	99,88	99,88	99,30	99,30	99,42	98,95	98,95	98,95	99,19	99,65	99,65		2	5
P11P2	16	99,30	99,30	99,65	99,65	99,65	99,07	99,07	99,19	98,72	98,72	98,72	98,95	99,42	99,42	99,77		7
SHIVC109consensus	17	99,19	99,19	99,53	99,30	99,30	99,65	99,65	99,77	98,84	98,84	99,07	99,30	99,30	99,30	99,42	99,19	

B: Control group animals

		1	2	3	4	5	6	7	8	9	10	11	12	13	14	15	16
P70i1	1		1	11	11	12	11	12	11	11	11	11	13	10	354	354	10
P70i2	2	99,88		12	12	13	12	13	12	12	12	12	14	11	355	355	11
P72i1	3	98,72	98,60		0	1	0	1	0	0	0	0	4	5	349	349	7
P72i2	4	98,72	98,60	100,00		1	0	1	0	0	0	0	4	5	349	349	7
P72i3	5	98,60	98,49	99,88	99,88		1	0	1	1	1	1	5	6	349	349	8
P72i4	6	98,72	98,60	100,00	100,00	99,88		1	0	0	0	0	4	5	349	349	7
P72i5	7	98,60	98,49	99,88	99,88	100,00	99,88		1	1	1	1	5	6	349	349	8
P72i6	8	98,72	98,60	100,00	100,00	99,88	100,00	99,88		0	0	0	4	5	349	349	7
P72i7	9	98,72	98,60	100,00	100,00	99,88	100,00	99,88	100,00		0	0	4	5	349	349	7
P72i8	10	98,72	98,60	100,00	100,00	99,88	100,00	99,88	100,00	100,00		0	4	5	349	349	7
P72i9	11	98,72	98,60	100,00	100,00	99,88	100,00	99,88	100,00	100,00	100,00		4	5	349	349	7
P72i10	12	98,49	98,37	99,53	99,53	99,42	99,53	99,42	99,53	99,53	99,53	99,53		9	353	353	11
P67P2	13	98,84	98,72	99,42	99,42	99,30	99,42	99,30	99,42	99,42	99,42	99,42	98,95		352	352	6
SHIVC109consensus	16	98,84	98,72	99,19	99,19	99,07	99,19	99,07	99,19	99,19	99,19	99,19	98,72	99,30	61,85	61,85	

C: Comparison of viral isolates from PBMCs of P4, P11 (vaccine group) and P67 (control group).

		1	2	3	4	5	6	7	8
P4P1	1		0	3	5	0	352	352	6
P4P2	2	100,00		3	5	0	352	352	6
P11P1	3	99,65	99,65		2	3	351	351	5
P11P2	4	99,42	99,42	99,77		5	351	351	7
P67P2	5	100,00	100,00	99,65	99,42		352	352	6
SHIVC109consensus	8	99,30	99,30	99,42	99,19	99,30	61,85	61,85	

D: Comparison of viral isolates from inguinal tissues of P25 (vaccine group) and P72 (control group).

		1	2	3	4	5	6	7	8	9	10	11	12	13	14	15	16
P25i1	1		0	1	7	7	8	8	9	8	9	8	8	8	8	12	3
P25i2	2	100,00		1	7	7	8	8	9	8	9	8	8	8	8	12	3
P25i3	3	99,88	99,88		8	8	7	7	8	7	8	7	7	7	7	11	2
P25i4	4	99,19	99,19	99,07		6	11	11	12	11	12	11	11	11	11	13	10
P25i5	5	99,19	99,19	99,07	99,30		11	11	12	11	12	11	11	11	11	13	10
P72i1	6	99,07	99,07	99,19	98,72	98,72		0	1	0	1	0	0	0	0	4	7
P72i2	7	99,07	99,07	99,19	98,72	98,72	100,00		1	0	1	0	0	0	0	4	7
P72i3	8	98,95	98,95	99,07	98,60	98,60	99,88	99,88		1	0	1	1	1	1	5	8
P72i4	9	99,07	99,07	99,19	98,72	98,72	100,00	100,00	99,88		1	0	0	0	0	4	7
P72i5	10	98,95	98,95	99,07	98,60	98,60	99,88	99,88	100,00	99,88		1	1	1	1	5	8
P72i6	11	99,07	99,07	99,19	98,72	98,72	100,00	100,00	99,88	100,00	99,88		0	0	0	4	7
P72i7	12	99,07	99,07	99,19	98,72	98,72	100,00	100,00	99,88	100,00	99,88	100,00		0	0	4	7
P72i8	13	99,07	99,07	99,19	98,72	98,72	100,00	100,00	99,88	100,00	99,88	100,00	100,00		0	4	7
P72i9	14	99,07	99,07	99,19	98,72	98,72	100,00	100,00	99,88	100,00	99,88	100,00	100,00	100,00		4	7
P72i10	15	98,60	98,60	98,72	98,49	98,49	99,53	99,53	99,42	99,53	99,42	99,53	99,53	99,53	99,53		11
SHIVC109consensus	16	99,65	99,65	99,77	98,84	98,84	99,19	99,19	99,07	99,19	99,07	99,19	99,19	99,19	99,19	98,72	

Figure 3. 11: Pairwise comparisons showing the percentage similarity and number of differing amino acids in sequences obtained from vaccinated and control group macaques. A all the sequences obtained from the vaccine group animals for both the inguinal tissue and PBMC. B sequences from control group macaques P70, P72 and P67. The sequences from P70 and P72 were obtained from inguinal tissue whereas P67 sequences were obtained from the PBMC. C a comparison between P4 and P11, vaccine group, and P67, control group, and the sequences obtained from the PBMC from these respective animals. D a comparison of sequences isolated from inguinal tissues between the vaccine group animal P25 and the control group animal P72. P following the number of the macaque = PBMC and i = inguinal tissue. The last number indicates the number of sequences obtained from that tissue sample.

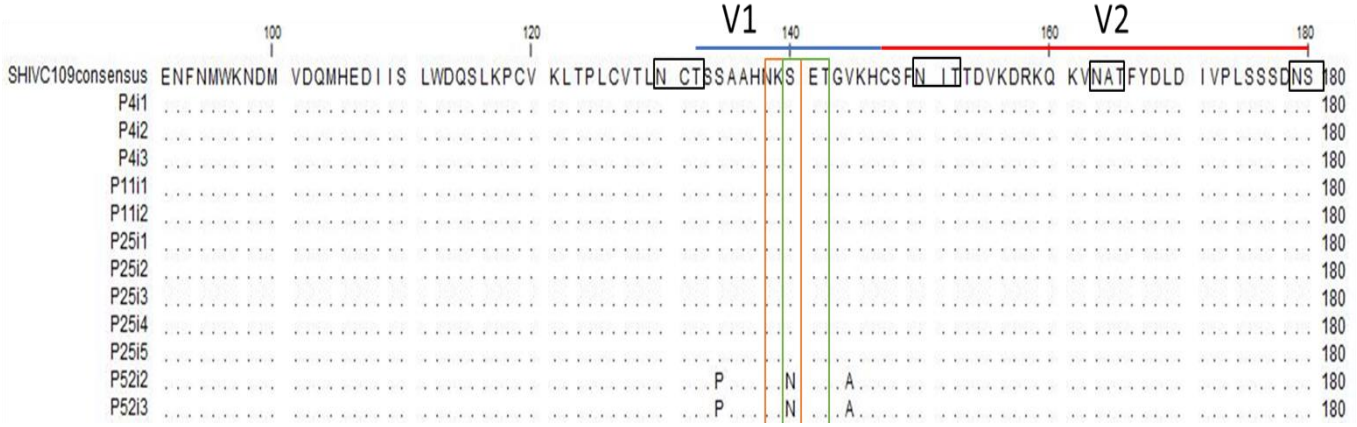

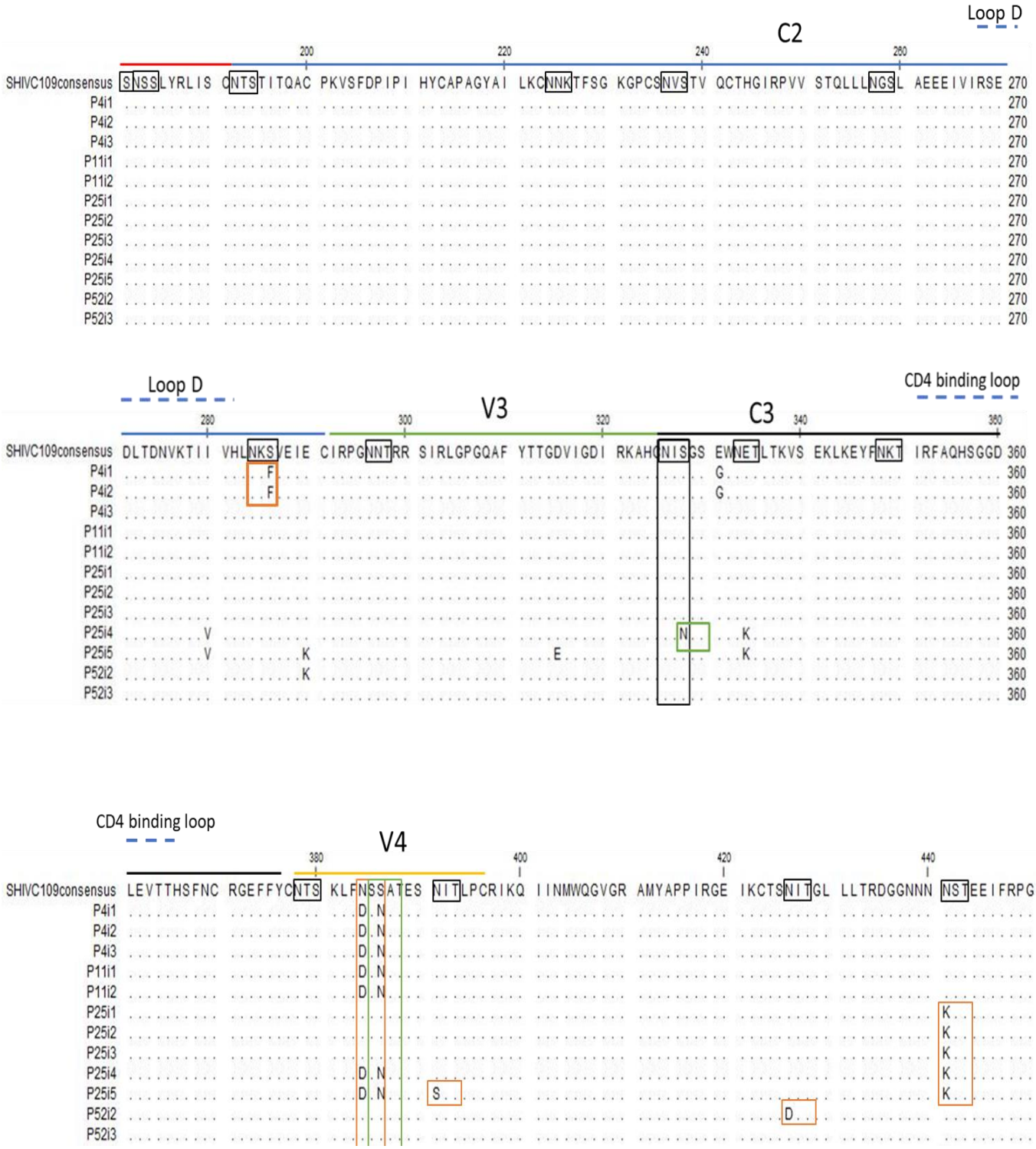

Figure 3. 12: Amino acid alignment of gp120 sequences from SHIV clones isolated from vaccinated macaques: Black boxes indicate potential N-glycosylation sites (PNGS), orange boxes indicate where glycosylation sites have been lost, and green boxes indicate where new sites have been gained. Above the sequences are shown the variable (V) and conserved (C) regions. **SHIVC109consensus = consensus sequence of challenge virus SHIVC109P7.**


V1
V2
Loop D
C2
Loop D
V3
C3
CD4 binding loop
SHIVC109consensus
P70i1
P70i2
P72i1
P72i2
P72i3
P72i4
P72i5
P72i6
P72i7
P72i8
P72i9
P72i10
P4P1
P4P2
P11P1
P11P2
P67P1
P67P2
P67P3

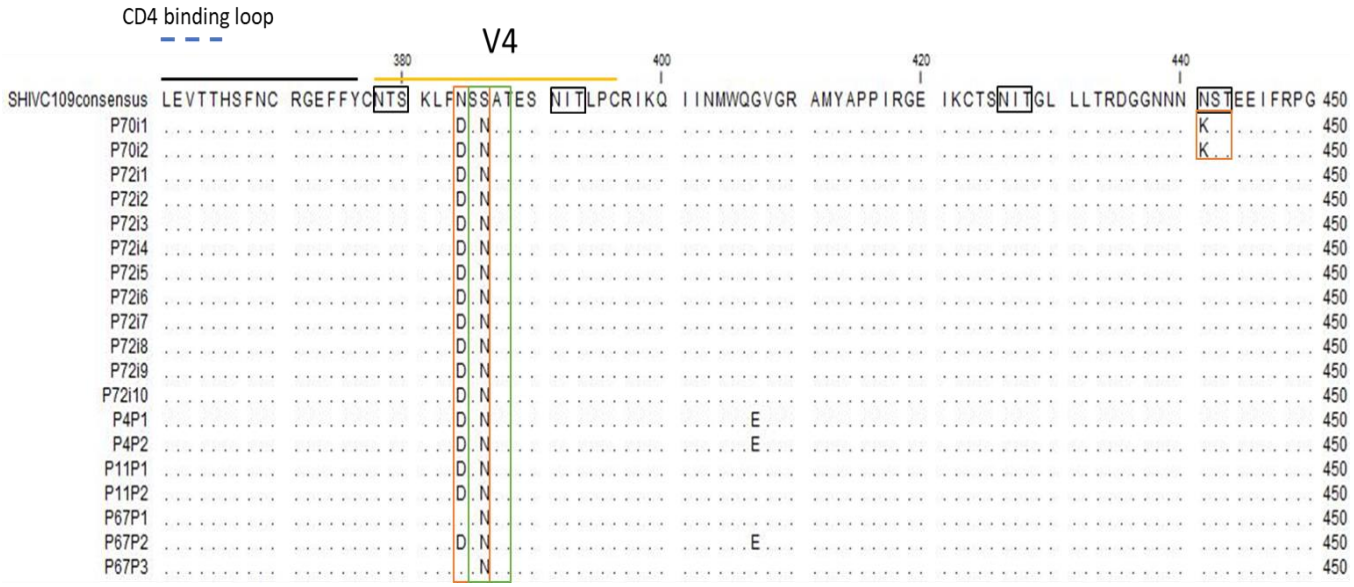

Figure 3. 13: Amino acid alignment of gp120 sequences from SHIV clones isolated from control macaques. Black boxes indicate potential N-glycosylation sites (PNGS), orange boxes indicate where glycosylation sites have been lost, green boxes indicate where new sites have been gained, and the blue box indicates an undetermined or atypical amino acid which can occurs when the original sequence quality is low or multiple sequences show different amino acids. Above the sequences are shown the variable (V) and conserved (C) regions. Loop D and CD4 binding loop also indicated by dashed lines. **SHIVC109consensus = consensus sequence of challenge virus SHIVC109P7.**

Discussion

The HIV viral reservoir is the main impediment to an HIV cure, as HIV can effectively evade the immune system by remaining dormant in infected T-lymphocyte cells. HIV is also capable of evading drugs as ART currently in use is only effective against actively replicating virus. This paired with the poor drug penetration in potential reservoir sites has led to difficulty in development of an HIV cure. Results from studies involving SIV macaque models as well as human clinical studies have led to an increased interest in functional cures and HIV eradication

(105-107). While a sterilizing cure is the main goal in curing HIV, a partially effective functional cure would have an impact on reducing HIV transmission by limiting the number of individuals with actively replicating HIV. If administered early enough a functional cure would also have the aim of limiting the size of the viral reservoir. Therefore, this study investigated the impact that the vaccination in rhesus macaques had on the formation of viral reservoirs.

The first study objective that was completed was the determination of RNA viral loads and proviral DNA in macaque tissues. Four out of five vaccine animals in this study had detectable PBMC RNA viral loads while only one of the four control animals had detectable PBMC RNA viral loads. All macaques had detectable inguinal RNA viral loads at the time of necropsy which was between 18- and 21-weeks post-infection. Similar results were seen for mesenteric RNA viral loads and splenocytes as all animals, except P47 from whom mesenteric samples could not be obtained, had detectable viral RNA loads 18 to 21 weeks post-infection. In a study by Kline et al viral loads in the PBMC remained low in pigtailed macaques that were infected with RT-SHIV$_{mne}$. PBMC viral loads remained low in macaques that were treated with ART as well as those that remained untreated. Two of the six untreated pigtailed macaques had detectable PBMC viral loads and only one of the six ART treated macaques had a detectable PBMC viral load. At least 50% of the untreated pigtailed macaques had detectable viral loads for the splenocytes, mesenteric and inguinal lymph nodes while one treated macaque had a detectable viral load for inguinal lymph nodes and two macaques had detectable viral loads for the spleen (81). In the Kline study as well as this study PBMC viral loads were lower than mesenteric and, inguinal lymph nodes and the splenocytes. Statistical analyses used in this experiment showed that there was no significant difference in viral loads between vaccinated and unvaccinated macaques. In a study conducted by the Chege et al RNA viral loads became undetectable by 6 -12 weeks post infection and remained undetectable for the remaining 36 months of the experimental period. Viral RNA levels obtained from cryo-preserved tissues

were also detected in the spleens of 5 of 10 animals (94). Statistical analyses were used to determine whether there was an RNA viral load difference between vaccinated and unvaccinated macaques within the same tissue groups. The lack of a significant difference means that the vaccine had no effect on the RNA viral loads of the macaques. A potential drawback on using cryopreserved samples for both the RNA and proviral DNA assays, is the possible degradation of both the RNA and DNA, during the thawing process. Cryopreservation reduces chemical reactions that occur within the cells which aids in long-term preservation. The formation of ice crystals, however, contributes to the degradation of RNA in tissue samples. RNA in tissues can also be degraded after multiple freezing and thawing cycles due to the action of RNAase. Another factor which could affect the average viral load is the difference in age between the vaccinated and control animals. The control animals were younger with healthier immune systems when compared to the vaccinated animals. The average viral load appeared higher in the vaccinated macaques but a couple animals which were outliers impacted the mean viral load as a result. Major histocompatibility complex (MHC) genotypes of the macaques could also impact on the susceptibility to infection; therefore, MHC genotyping is planned for future work (95).

Proviral DNA was present in all animals at detectable levels 18-21 weeks post-infection, the presence of proviral DNA in PBMC cells as well as in inguinal and mesenteric lymph tissues and splenocytes is an indicator of viral reservoirs present in the macaques. Similar to other studies, proviral DNA levels were measurable meaning that viral reservoirs were present in those tissue sites. There was no conclusive lymph tissue which had the highest levels of proviral DNA or viral RNA which is in contrast to some studies where mesenteric lymph nodes had both the highest proviral DNA levels as well as the highest levels of SIV gag RNA (108, 109). Proviral DNA was measured in the spleen and lymph nodes of macaques in the Chege study

confirming the presence of a latent viral reservoir in these tissues (94). Statistical analyses were used to determine whether there was a difference in the proviral DNA load between vaccinated and unvaccinated macaques within the same tissue groups. The lack of a significant difference suggests that the vaccine had no effect on the proviral DNA viral loads of the macaques and was not able to affect the seeding of the reservoir which occurs very early during infection. Further ELISAs such as the quantitative viral outgrowth assay should be included in further studies as it is useful to know how much of the latent reservoir is replication competent and how much of the reservoir consists of defective provirus. Determining whether a vaccine has an effect on the percentage of defective provirus present in the reservoir would be an interesting question to answer and is an avenue that should be pursued in the future.

The next completed objective was to determine whether the macaques developed binding antibodies to SHIV Env and Gag antigens through a Western blotting assay. All macaques had detectable binding antibodies to HIV Env and SIV Gag. For all vaccine group macaques, the levels of Env antibodies seem to increase from week 13 to 32 and then either plateau or slightly decrease at week 53. Levels of Env antibodies increased from week 13 to 32 as the protein vaccine boosts the Env titres. For macaques P4, P11, P25 and, P47 the Gag antibodies appeared to be their highest at week 13 and gradually decline at week 32 and 53. P52 appeared to have minimal Gag antibodies at week 13, but the titre appeared to have increased at week 53. For macaques P4, P11 and P25 the Gag antibody titres appear to be higher than the Env antibody titres at week 13 one-week post MVA inoculation. At weeks 32 and 53, 4 weeks post protein inoculation and at necropsy, the Env antibody titre appear to be higher than the Gag antibody titres. To reduce the background present in the Western blots cell lysates from cells transfected with DNA vaccines expressing HIV-1 Env and SIV Gag could be used in further experiments. These cell lysates could produce Western blots with less background. The cell lysates used in this experiment were from cells infected with MVA and produced background as more

antibodies were generated to MVA and non-specific proteins in the vaccine preparation in the macaques than the DNA vaccines would have.

Once it was determined through the Western blots that the macaques had binding antibodies to HIV-1 Env, ELISA assays were used to quantify the levels of binding antibodies. The ELISA assays ultimately did corroborate the results of the Western blots with binding antibody titres being present in the plasma of the macaques at all the timepoints tested on the Western blots. Vaccine group macaques all generated gp140-specific binding antibodies following immunizations. All vaccine group macaques except P11 reached their peak binding antibody titre at week 22 (after the first protein boost) whereas macaque P11 reached its peak at week 30 (after second protein boost; Figure 3.10). Prior to reaching their peaks at week 22 macaques P4, P25, P47 and P52 had a steady increase in binding antibody titres from week 6 up to week 22. Macaque P11 saw a decrease in binding antibody titres between week 6 and week 13 (Figure 3.10). Control group macaques also generated gp140-specific binding antibodies following SHIV challenge as they were present at the time of euthanasia. In another study macaques were given two DNA priming injections spaced by two months followed by a four-month interval and then three gp140 protein boosts, spaced by two-month intervals ((110)). The protein boost was administered with three different adjuvants. All the macaques developed gp140 specific antibody responses two weeks after the first protein immunization. This differs from our study where two macaques, P4 and P11, did develop antibodies after the DNA vaccination. Between the protein immunizations there was a 10-fold decrease in antibody titres. (110). Similar to the Bowles et al study there was a 2-month period between protein inoculations used in this study. There was not a 10-fold decrease between the protein immunizations however three of the five macaques show have a decrease in binding antibody titres between week 22 which is two weeks post the first protein inoculation and week 30 which

is two week post the second protein inoculation (Figure 3.9 and Figure 3.10). Binding antibody titres at week 53, day of euthanasia, obtained for the vaccinated and control macaques were very similar with only one vaccinated macaque P52 having a higher binding antibody titre than a control animal. Vaccinated macaques P4, P11, P25, and P47 had the same binding antibody titres as control group macaques P67 and P70. P52 and P71 had the same binding antibody titre whereas P72 had the largest binding antibody titre out of all the animals. Of the vaccine animals only macaque P25 required one challenge to become infected whereas P4, P11, P47, and P52 required two challenges to become infected. Antibody titres at week 32, day of first challenge, do not vary greatly with macaque P4 having the largest titre while macaques P11, P25, P47 and P52 had the same titres. There was a 4-fold difference between the titres of these animals at week 32. The titres at week 32 do not seem to have had an effect on the number of challenges it took to become infected. A virus neutralization assay to determine whether the macaques developed neutralizing antibodies and at what time points these antibodies are present could be performed in future experiments.

The final completed objective was the isolation and sequencing of the envelope gene of viruses obtained from inguinal tissue and PBMC. What was observed in the sequences for the macaques used in this study is that there were very few differences in amino acids resulting in sequences that were approximately 98% similar to any other sequence regardless of where the sequences were isolated from or whether the macaque was vaccinated or in the control group. The sequences showed changes to potential N-linked glycosylation sites (PNGS) in the variable region 1 (V1), N326 in the conserved region (C3) and variable region 4 (V4) had occurred in some of the clones. Increased replication and the potential to deplete CD4 cells have been described as a result of amino acid alterations in Env glycoproteins(94). When comparing the changes to PNGS 11 of 13 control group macaques had changes to the PNG at position 140 whereas only 2 of 14 vaccine group macaques had changes at this position. PNGs were also

lost at position 284 for the P4I, position 391 for P25I5, position 426 for P52I2, and position 441 for 4 of the vaccine group animal sequences and 2 of the control group. In total there were 22 lost PNGs in the vaccine group sequences and 29 lost PNG in the control group sequences. At location 394 there were changes to the PNG for a majority of both groups of macaques. At certain PNG locations for the control and vaccine group macaques it seems like the virus sequence is returning to the sequence in SHIVC109P4 (94). Similar studies have been conducted by (109) whereby they have looked at viral reservoirs in Chinese macaques this study differs in that the monkeys were not infected with a SIV virus but with a SHIV virus. Siddiqui et al also looked at reservoir formation with regards to suppressive antiretroviral therapy whereas this study is looking at reservoirs with regards to vaccinated macaques. Studies looking at the time of HIV reservoir formation have also been done by (67) but this has been done with a human cohort with a focus on viral sequencing. Similar to Siddiqui et al low levels of PBMC viral loads led to very few sequences being isolated. Prior to their selection for which tissues to use for sequencing they sequenced PBMCs at day 14 and day 30 post infection. Overall, the result of the sequencing shows that regardless of where the sequences were isolated from, inguinal or PBMC, or vaccinated or not very few amino acid changes occurred. As early viruses are vital in the formation of the viral reservoir it could explain the lack of changes in sequences obtained from different tissue sites. Sequences obtained at peak viremia might therefore contain more variation as the viruses are actively replicating. Further sequencing analysis can be performed in the future as there are further lymphoid tissues which have been harvested but sequences have not been isolated yet due to time and funding constraints.

Overall, this study shows that the vaccination had no effect on the size or distribution of the viral reservoir. The proviral DNA assay showed that there was no significant difference between the control and vaccine group within tissue groups meaning that the vaccine did not

have an effect on the size or distribution of the viral reservoir. The vaccine also had no major effect on the variability of the viruses present in the reservoir which can be seen by the lack of sequence variability present in the sequences. The aims of this experiment were ultimately met and provides a good platform for investigating tissues which have not been used in this study. By using more tissues in this study more information can be obtained regarding the viral reservoir and the impact vaccination has on it. Observing the viral sequences and its potential changes over a longer period of time would increase understanding of when the reservoir forms and the changes that occur within these reservoirs over time.

Appendix

A. Isolation of Peripheral blood mononuclear cells (PBMCs) from whole blood

Heparinised whole blood was obtained from SHIV-infected macaques and PBMCs were isolated using Ficoll-HistoPaque™ density gradient centrifugation (Sigma-Aldrich). Fifteen mL of room temperature Ficoll was pipetted into 50 mL LeucosepTM separation tubes (LST) (Lasec) containing a separation filter and centrifuged for one minute at 1000 *g* to allow the Ficoll to pass below the separation filter. A volume of 10 to 25mL of whole blood was then layered onto the separation disk of the LST and centrifuged for 10 minutes at 1000 *g* to separate the blood into distinct layers. Plasma was collected and aliquoted into 2-mL microtubes and stored at -20 °C. The PBMC layer was then transferred into a clean 50 mL centrifuge tube and diluted to 50 mL using PBMC wash solution (1% heat inactivated foetal bovine serum (Biochrom) in PBS (Gibco). Cells were then pelleted by centrifugation at 250 *g* for 10 minutes. The supernatant was then removed without disturbing the pellet. The pellet was then resuspended in 10-40 mL of PBMC wash solution. Cells were then manually counted using both Trypan blue dye and Turk's solution. Following the cell counting, the cells were pelleted and resuspended in cryopreserving media of FBS with 10% DMSO at a concentration of 10 million cells per mL. Aliquots of cells were stored in liquid nitrogen.

B. Isolation of mononuclear cells (MNC) from lymph nodes

Isolation of MNC from lymph nodes

Whole lymph nodes obtained at necropsy was put into a 50 mL tube containing 15 mL R5 media and stored on wet ice while being transported to the lab. Once at the lab the contents of the tube were poured into a Petri dish. The media was then removed, and the tissue surfaces were washed with ice-cold R5 media. Fatty tissues were then removed, and the tissue was transferred into another Petri dish containing R5. The tissue was then lacerated by making several cuts on the surface with a scalpel blade to disrupt the tissue coating. Mesenchymal tissues were teased out by scraping with a blade on the surface while holding the tissue with forceps. The coating was then removed and discarded. The contents were then aspirated with a pipette into a 50 mL tube via a 70-micron filter. The Petri dish was then washed once with 10 mL of R5. The R5 used to wash the Petri dish was then added to the tube via the filter. Centrifuge at 250 *g* for 10 minutes at toom temperature and resuspend the pellet in 10 mL fresh R10. The collected cells were kept at room temperature. For each lymph node harvest the cell count and cell viability was performed using a haemocytometer and microscope (10 μL cell suspension plus 90 μL Trypan blue solution). Cells are then cryo-preserved.

Isolation of splenocytes

A section of spleen obtained at necropsy was put into a 50 mL tube containing 15 mL R5 media and stored on wet ice while being transported to the lab. Once at the lab the contents of the tube were poured into a Petri dish. The media was then removed, the tissue surfaces were washed with ice-cold R5 media and connective tissues were cut away before being transferred into another Petri dish containing R5. The tissue was then lacerated by making several cuts on the surface with a scalpel blade to disrupt the tissue coating. Using the rubber portion of a 2 mL or 5 mL syringe piston grind the mesenchymal tissues into a fine pulp. Remove and discard the

connective tissue coatings. Aspirate and the eject the contents via a fine-bore needle and syringe a few times to further disrupt the tissues. The tissues are then transferred into a 50 mL tube via 70-micron filter. The Petri dish was then washed with 10 mL R5. The R5 used to wash the Petri dish was then added to the tube via the filter. The tube was then centrifuged at 250 *g* for 10 minutes at room temperature. The pellet was then resuspended in 2 ml ammonium chloride solution (lysing solution) and incubated for 2 minutes at room temperature. The tube was the topped up with R5 to 50 mL and twice centrifuged at 250 *g* for 10 minutes. The cell count and cell viability were performed using a haemocytometer and microscope (10 μL cell suspension plus 90 μL Trypan blue solution). Cells are then cryo-preserved.

C. Buffers, Media and Solutions.

Ponceau S Solution (100ml)

Ponceau S	2g
Trichloroacetic acid	30g
5-sulfosalicyclic acid	30g
Water	adjust to 100 mL

Prepare working stock by diluting 10 times.

Protein transfer buffer

Trizma-base	5.82 g
Glycine	2.93 g
100% Methanol	200 mL
Water	adjust to 1000 mL

Block / Wash Buffer

Instant milk powder	40 g
Tween-20	5 mL

1X PBS	up to 1000 mL

4X Protein loading dye (Laemmli buffer)

Glycerol	4 mL
1.5M Tris-HCL pH 6.8	1.6 mL
Bromophenol blue	4 mg
SDS powder	0. 8 g
Beta-mercaptoethanol	0.5 mL
RO H_20	3.9 mL

10X SDS Running Buffer

SDS	10 g
Tris	30.3 g
Glycine	29 g
RO H2O	adjust to 1000 mL

Dilute to 1X with RO H2O when needed

8% Resolving gel (two gels)

H_20	5.3 mL
40% Bis-Acrylamide	2 mL
1.5M Tris-HCL pH 8.8	2.5 mL
10% SDS	0.1 mL
10% Ammonium persulfate APS	0.1 mL
TEMED	6 µl

4% Stacking gel (two gels)

H_20	3.8 mL
40% Bis-Acrylamide	0.5 mL
1.5M Tris-HCL pH 6.8	0.63 mL
10% SDS	50 µL
10% Ammonium persulfate APS	50 µL
TEMED	5 µL

References

1. UNAIDS. 2019 UNAIDS data [Available from: https://www.unaids.org/sites/default/files/media_asset/2019-UNAIDS-data_en.pdf.
2. Vandormael A, Akullian A, Siedner M, de Oliveira T, Bärnighausen T, Tanser F. Declines in HIV incidence among men and women in a South African population-based cohort. Nature Communications. 2019;10(1):5482.
3. Robinson HL. HIV/AIDS Vaccines: 2018. Clin Pharmacol Ther. 2018;104(6):1062-73.
4. Lema D, Garcia A, De Sanctis JB. HIV Vaccines: A Brief Overview. Scandinavian Journal of Immunology. 2014;80(1):1-11.
5. Zolla-Pazner S, Gilbert PB, Simon V. Revisiting the Correlate of Reduced HIV Infection Risk in the Rv144 Vaccine Trial. Journal of Virology. 2019;93(17):e00629-19.
6. Brown KC, Paul S, Kashuba ADM. Drug interactions with new and investigational antiretrovirals. Clin Pharmacokinet. 2009;48(4):211-41.
7. Permanyer M, Ballana E, Ruiz A, Badia R, Riveira-Munoz E, Gonzalo E, et al. Antiretroviral Agents Effectively Block HIV Replication after Cell-to-Cell Transfer. Journal of Virology. 2012;86(16):8773.
8. Sluis-Cremer N, Arion D, Parniak* MA. Molecular mechanisms of HIV-1 resistance to nucleoside reverse transcriptase inhibitors (NRTIs). Cellular and Molecular Life Sciences CMLS. 2000;57(10):1408-22.
9. Trinité B, Zhang H, Levy DN. NNRTI-induced HIV-1 protease-mediated cytotoxicity induces rapid death of CD4 T cells during productive infection and latency reversal. Retrovirology. 2019;16(1):17.
10. Hajimahdi Z, Zarghi A. Progress in HIV-1 Integrase Inhibitors: A Review of their Chemical Structure Diversity. Iran J Pharm Res. 2016;15(4):595-628.
11. Marathe KR, Patil RH, Vishwakarma KS, Chaudhari AB, Maheshwari VL. Chapter 6 - Protease Inhibitors and Their Applications: An Overview. In: Atta ur R, editor. Studies in Natural Products Chemistry. 62: Elsevier; 2019. p. 211-42.
12. Qian K, Morris-Natschke SL, Lee KH. HIV entry inhibitors and their potential in HIV therapy. Med Res Rev. 2009;29(2):369-93.
13. Ehrenberg PK, Shangguan S, Issac B, Alter G, Geretz A, Izumi T, et al. A vaccine-induced gene expression signature correlates with protection against SIV and HIV in multiple trials. Science Translational Medicine. 2019;11.
14. Younai FS. Thirty years of the human immunodeficiency virus epidemic and beyond. International Journal of Oral Science. 2013;5(4):191-9.
15. Leite TF, Delatorre E, Côrtes FH, Ferreira ACG, Cardoso SW, Grinsztejn B, et al. Reduction of HIV-1 Reservoir Size and Diversity After 1 Year of cART Among Brazilian Individuals Starting Treatment During Early Stages of Acute Infection. Frontiers in Microbiology. 2019;10:145.
16. Kearney MF, Spindler J, Shao W, Yu S, Anderson EM, O'Shea A, et al. Lack of Detectable HIV-1 Molecular Evolution during Suppressive Antiretroviral Therapy. PLOS Pathogens. 2014;10(3):e1004010.
17. Dufloo J, Bruel T, Schwartz O. HIV-1 cell-to-cell transmission and broadly neutralizing antibodies. Retrovirology. 2018;15(1):51.
18. Lelièvre J-D, Lévy Y. HIV-1 prophylactic vaccines: state of the art. J Virus Erad. 2016;2(1):5-11.
19. Martinez-Picado J, Deeks SG. Persistent HIV-1 replication during antiretroviral therapy. Curr Opin HIV AIDS. 2016;11(4):417-23.

20. Feinberg MB, Greene WC. Molecular insights into human immunodeficiency virus type 1 pathogenesis. Curr Opin Immunol. 1992;4(4):466-74.
21. Campbell EM, Hope TJ. HIV-1 capsid: the multifaceted key player in HIV-1 infection. Nat Rev Microbiol. 2015;13(8):471-83.
22. German Advisory Committee Blood SAoPTbB. Human Immunodeficiency Virus (HIV). Transfus Med Hemother. 2016;43(3):203-22.
23. Lu K, Heng X, Summers MF. Structural determinants and mechanism of HIV-1 genome packaging. J Mol Biol. 2011;410(4):609-33.
24. Chakraborty S, Rahman T, Chakravorty R. Characterization of the Protective HIV-1 CTL Epitopes and the Corresponding HLA Class I Alleles: A Step towards Designing CTL Based HIV-1 Vaccine. Adv Virol. 2014;2014:321974.
25. Cochrane A. HIV-1 Rev function and RNA nuclear-cytoplasmic export. Methods Mol Biol. 2014;1087:103-14.
26. Rice AP. The HIV-1 Tat Protein: Mechanism of Action and Target for HIV-1 Cure Strategies. Curr Pharm Des. 2017;23(28):4098-102.
27. Blissenbach M, Grewe B, Hoffmann B, Brandt S, Überla K. Nuclear RNA Export and Packaging Functions of HIV-1 Rev Revisited. Journal of Virology. 2010;84(13):6598.
28. Li G, De Clercq E. HIV Genome-Wide Protein Associations: a Review of 30 Years of Research. Microbiology and Molecular Biology Reviews. 2016;80(3):679.
29. Kogan M, Rappaport J. HIV-1 Accessory Protein Vpr: Relevance in the pathogenesis of HIV and potential for therapeutic intervention. Retrovirology. 2011;8(1):25.
30. González ME. Vpu Protein: The Viroporin Encoded by HIV-1. Viruses. 2015;7(8):4352-68.
31. Reddy K, Ooms M, Letko M, Garrett N, Simon V, Ndung'u T. Functional characterization of Vif proteins from HIV-1 infected patients with different APOBEC3G haplotypes. AIDS. 2016;30(11):1723-9.
32. Bergamaschi A, Ayinde D, David A, Le Rouzic E, Morel M, Collin G, et al. The Human Immunodeficiency Virus Type 2 Vpx Protein Usurps the CUL4A-DDB1^{DCAF1} Ubiquitin Ligase To Overcome a Postentry Block in Macrophage Infection. Journal of Virology. 2009;83(10):4854.
33. Felli C, Vincentini O, Silano M, Masotti A. HIV-1 Nef Signaling in Intestinal Mucosa Epithelium Suggests the Existence of an Active Inter-kingdom Crosstalk Mediated by Exosomes. Frontiers in Microbiology. 2017;8.
34. Freed EO. HIV-1 assembly, release and maturation. Nature Reviews Microbiology. 2015;13(8):484-96.
35. Deeks SG, Overbaugh J, Phillips A, Buchbinder S. HIV infection. Nature Reviews Disease Primers. 2015;1(1):15035.
36. Okoye AA, Picker LJ. CD4(+) T-cell depletion in HIV infection: mechanisms of immunological failure. Immunol Rev. 2013;254(1):54-64.
37. Loftin LM, Kienzle M, Yi Y, Collman RG. R5X4 HIV-1 coreceptor use in primary target cells: implications for coreceptor entry blocking strategies. J Transl Med. 2011;9 Suppl 1(Suppl 1):S3.
38. Dimitrov AS, Louis JM, Bewley CA, Clore GM, Blumenthal R. Conformational changes in HIV-1 gp41 in the course of HIV-1 envelope glycoprotein-mediated fusion and inactivation. Biochemistry. 2005;44(37):12471-9.
39. Frankel AD, Young JAT. HIV-1: Fifteen Proteins and an RNA. Annual Review of Biochemistry. 1998;67(1):1-25.
40. Keller PW, Morrison O, Vassell R, Weiss CD. HIV-1 gp41 Residues Modulate CD4-Induced Conformational Changes in the Envelope Glycoprotein and Evolution of a Relaxed Conformation of gp120. J Virol. 2018;92(16).
41. Yamashita M, Engelman AN. Capsid-Dependent Host Factors in HIV-1 Infection. Trends Microbiol. 2017;25(9):741-55.

42. Anderson EM, Maldarelli F. The role of integration and clonal expansion in HIV infection: live long and prosper. Retrovirology. 2018;15(1):71.
43. Craigie R, Bushman FD. HIV DNA integration. Cold Spring Harb Perspect Med. 2012;2(7):a006890.
44. Roebuck KA, Saifuddin M. Regulation of HIV-1 transcription. Gene Expr. 1999;8(2):67-84.
45. Karn J, Stoltzfus CM. Transcriptional and posttranscriptional regulation of HIV-1 gene expression. Cold Spring Harb Perspect Med. 2012;2(2):a006916.
46. Wu Y, Marsh JW. Gene transcription in HIV infection. Microbes and Infection. 2003;5(11):1023-7.
47. Checkley MA, Luttge BG, Freed EO. HIV-1 envelope glycoprotein biosynthesis, trafficking, and incorporation. J Mol Biol. 2011;410(4):582-608.
48. Parent LJ, Gudleski N. Beyond plasma membrane targeting: role of the MA domain of Gag in retroviral genome encapsidation. J Mol Biol. 2011;410(4):553-64.
49. Ganser-Pornillos BK, Yeager M, Sundquist WI. The structural biology of HIV assembly. Current Opinion in Structural Biology. 2008;18(2):203-17.
50. Kariuki SM, Selhorst P, Ariën KK, Dorfman JR. The HIV-1 transmission bottleneck. Retrovirology. 2017;14(1):22-.
51. Cohen MS, Gay CL, Busch MP, Hecht FM. The Detection of Acute HIV Infection. The Journal of Infectious Diseases. 2010;202(Supplement_2):S270-S7.
52. O'Brien SP, Swanstrom AE, Pegu A, Ko S-Y, Immonen TT, Del Prete GQ, et al. Rational design and in vivo selection of SHIVs encoding transmitted/founder subtype C HIV-1 envelopes. PLOS Pathogens. 2019;15(4):e1007632.
53. Chen Z, Huang Y, Zhao X, Skulsky E, Lin D, Ip J, et al. Enhanced Infectivity of an R5Tropic Simian/Human Immunodeficiency Virus Carrying Human Immunodeficiency Virus Type 1 Subtype C Envelope after Serial Passages in Pig-Tailed Macaques (Macaca nemestrina). Journal of Virology - J VIROL. 2000;74:6501-10.
54. Song RJ, Chenine AL, Rasmussen RA, Ruprecht CR, Mirshahidi S, Grisson RD, et al. Molecularly Cloned SHIV-1157ipd3N4: a Highly Replication- Competent, Mucosally Transmissible R5 Simian-Human Immunodeficiency Virus Encoding HIV Clade C <em>env</em&gt. Journal of Virology. 2006;80(17):8729.
55. Asmal M, Luedemann C, Lavine CL, Mach LV, Balachandran H, Brinkley C, et al. Infection of monkeys by simian-human immunodeficiency viruses with transmitted/founder clade C HIV-1 envelopes. Virology. 2015;475:37-45.
56. Sharma A, Boyd DF, Overbaugh J. Development of SHIVs with circulating, transmitted HIV-1 variants. Journal of Medical Primatology. 2015;44(5):296-300.
57. Akiyama H, Ishimatsu M, Miura T, Hayami M, Ido E. Construction and infection of a new simian/human immunodeficiency chimeric virus (SHIV) containing the integrase gene of the human immunodeficiency virus type 1 genome and analysis of its adaptation to monkey cells. Microbes and Infection. 2008;10(5):531-9.
58. Roark RS, Li H, Williams WB, Chug H, Mason RD, Gorman J, et al. Recapitulation of HIV-1 Env-antibody coevolution in macaques leading to neutralization breadth. Science. 2021;371(6525):eabd2638.
59. Malamba SS, Morgan D, Clayton T, Mayanja B, Okongo M, Whitworth J. The prognostic value of the World Health Organisation staging system for HIV infection and disease in rural Uganda. AIDS. 1999;13(18).
60. Naif HM. Pathogenesis of HIV Infection. Infect Dis Rep. 2013;5(Suppl 1):e6.
61. Simon V, Ho DD, Abdool Karim Q. HIV/AIDS epidemiology, pathogenesis, prevention, and treatment. The Lancet. 2006;368(9534):489-504.
62. Weinberg JL, Kovarik CL. The WHO Clinical Staging System for HIV/AIDS. Virtual Mentor [Internet]. 2010 2010; 12(3):[202-6 pp.]. Available from: http://europepmc.org/abstract/MED/23140869

https://doi.org/10.1001/virtualmentor.2010.12.3.cprl1-1003.
63. Karch CP, Matyas GR, Burkhard P, Beck Z. Glycosylation of the HIV-1 Env V1V2 loop to form a native-like structure may not be essential with a nanoparticle vaccine. Future Virology. 2019;14(2):51-4.
64. Stano A, Leaman DP, Kim AS, Zhang L, Autin L, Ingale J, et al. Dense Array of Spikes on HIV-1 Virion Particles. Journal of virology. 2017;91(14):e00415-17.
65. Ringel O, Vieillard V, Debré P, Eichler J, Büning H, Dietrich U. The Hard Way towards an Antibody-Based HIV-1 Env Vaccine: Lessons from Other Viruses. Viruses. 2018;10(4):197.
66. Mogensen TH, Melchjorsen J, Larsen CS, Paludan SR. Innate immune recognition and activation during HIV infection. Retrovirology. 2010;7(1):54.
67. Abrahams MR, Joseph SB, Garrett N, Tyers L, Moeser M, Archin N, et al. The replication-competent HIV-1 latent reservoir is primarily established near the time of therapy initiation. Sci Transl Med. 2019;11(513).
68. Jean MJ, Fiches G, Hayashi T, Zhu J. Current Strategies for Elimination of HIV-1 Latent Reservoirs Using Chemical Compounds Targeting Host and Viral Factors. AIDS Research and Human Retroviruses. 2018;35(1):1-24.
69. Vanhamel J, Bruggemans A, Debyser Z. Establishment of latent HIV-1 reservoirs: what do we really know? J Virus Erad. 2019;5(1):3-9.
70. McDermott AB, Mitchen J, Piaskowski S, De Souza I, Yant LJ, Stephany J, et al. Repeated low-dose mucosal simian immunodeficiency virus SIVmac239 challenge results in the same viral and immunological kinetics as high-dose challenge: a model for the evaluation of vaccine efficacy in nonhuman primates. J Virol. 2004;78(6):3140-4.
71. Shedlock DJ, Silvestri G, Weiner DB. Monkeying around with HIV vaccines: using rhesus macaques to define 'gatekeepers' for clinical trials. Nat Rev Immunol. 2009;9(10):717-28.
72. Sui Y, Gordon S, Franchini G, Berzofsky JA. Nonhuman primate models for HIV/AIDS vaccine development. Curr Protoc Immunol. 2013;102:12.4.1-.4.30.
73. Barouch DH, Stephenson KE, Borducchi EN, Smith K, Stanley K, McNally AG, et al. Protective efficacy of a global HIV-1 mosaic vaccine against heterologous SHIV challenges in rhesus monkeys. Cell. 2013;155(3):531-9.
74. Manrique M, Micewicz E, Kozlowski PA, Wang S-W, Aurora D, Wilson RL, et al. DNA-MVA vaccine protection after X4 SHIV challenge in macaques correlates with day-of-challenge antiviral CD4+ cell-mediated immunity levels and postchallenge preservation of CD4+ T cell memory. AIDS research and human retroviruses. 2008;24(3):505-19.
75. Willey RL, Byrum R, Piatak M, Kim YB, Cho MW, Rossio JL, et al. Control of Viremia and Prevention of Simian-Human Immunodeficiency Virus-Induced Disease in Rhesus Macaques Immunized with Recombinant Vaccinia Viruses plus Inactivated Simian Immunodeficiency Virus and Human Immunodeficiency Virus Type 1 Particles. Journal of Virology. 2003;77(2):1163.
76. Wong JK, Yukl SA. Tissue reservoirs of HIV. Curr Opin HIV AIDS. 2016;11(4):362-70.
77. Mzingwane ML, Tiemessen CT. Mechanisms of HIV persistence in HIV reservoirs. Reviews in Medical Virology. 2017;27(2):e1924.
78. Goonetilleke N, Clutton G, Swanstrom R, Joseph SB. Blocking Formation of the Stable HIV Reservoir: A New Perspective for HIV-1 Cure. Front Immunol. 2019;10:1966.
79. Horsburgh BA, Palmer S. For Viral Reservoir Studies, Timing Matters. Trends in Microbiology. 2019;27(10):809-10.
80. Bender AM, Simonetti FR, Kumar MR, Fray EJ, Bruner KM, Timmons AE, et al. The Landscape of Persistent Viral Genomes in ART-Treated SIV, SHIV, and HIV-2 Infections. Cell Host Microbe. 2019;26(1):73-85.e4.
81. Kline C, Ndjomou J, Franks T, Kiser R, Coalter V, Smedley J, et al. Persistence of Viral Reservoirs in Multiple Tissues after Antiretroviral Therapy Suppression in a Macaque RT-SHIV Model. PLOS ONE. 2013;8(12):e84275.

82. Deeks SG, Autran B, Berkhout B, Benkirane M, Cairns S, Chomont N, et al. Towards an HIV cure: a global scientific strategy. Nature Reviews Immunology. 2012;12(8):607-14.
83. Chen Z. Monkey Models and HIV Vaccine Research. Adv Exp Med Biol. 2018;1075:97-124.
84. Policicchio BB, Pandrea I, Apetrei C. Animal Models for HIV Cure Research. Front Immunol. 2016;7:12-.
85. Liu Z, Tan X, Orozco-terWengel P, Zhou X, Zhang L, Tian S, et al. Population genomics of wild Chinese rhesus macaques reveals a dynamic demographic history and local adaptation, with implications for biomedical research. GigaScience. 2018;7(9).
86. Zhou Y, Bao R, Haigwood NL, Persidsky Y, Ho W-z. SIV infection of rhesus macaques of Chinese origin: a suitable model for HIV infection in humans. Retrovirology. 2013;10(1):89.
87. Raehtz KD, Barrenas F, Xu C, Busman-Sahay K, Valentine A, Law L, et al. African green monkeys avoid SIV disease progression by preventing intestinal dysfunction and maintaining mucosal barrier integrity. PLoS Pathog. 2020;16(3):e1008333.
88. Pandrea I, Landay A, Wilson C, Stock J, Tracy R, Apetrei C. Using the pathogenic and nonpathogenic nonhuman primate model for studying non-AIDS comorbidities. Current HIV/AIDS reports. 2015;12(1):54-67.
89. Zhang XL, Pang W, Hu XT, Li JL, Yao YG, Zheng YT. Experimental primates and non-human primate (NHP) models of human diseases in China: current status and progress. Dongwuxue Yanjiu. 2014;35(6):447-64.
90. Hatziioannou T, Evans DT. Animal models for HIV/AIDS research. Nat Rev Microbiol. 2012;10(12):852-67.
91. Hessell AJ, Haigwood NL. Animal models in HIV-1 protection and therapy. Curr Opin HIV AIDS. 2015;10(3):170-6.
92. Klatt NR, Silvestri G, Hirsch V. Nonpathogenic simian immunodeficiency virus infections. Cold Spring Harb Perspect Med. 2012;2(1):a007153-a.
93. Ren W, Mumbauer A, Gettie A, Seaman MS, Russell-Lodrigue K, Blanchard J, et al. Generation of Lineage-Related, Mucosally Transmissible Subtype C R5 Simian-Human Immunodeficiency Viruses Capable of AIDS Development, Induction of Neurological Disease, and Coreceptor Switching in Rhesus Macaques. Journal of Virology. 2013;87(11):6137.
94. Chege GK, Adams CH, Keyser AT, Bekker V, Morris L, Villinger FJ, et al. Infection of Chinese Rhesus Monkeys with a Subtype C SHIV Resulted in Attenuated In Vivo Viral Replication Despite Successful Animal-to-Animal Serial Passages. Viruses. 2021;13(3):397.
95. Mommaerts K, Sanchez I, Betsou F, Mathieson W. Replacing β-mercaptoethanol in RNA extractions. Analytical Biochemistry. 2015;479:51-3.
96. Kralik P, Ricchi M. A Basic Guide to Real Time PCR in Microbial Diagnostics: Definitions, Parameters, and Everything. Frontiers in Microbiology. 2017;8(108).
97. Bustin SA, Nolan T. RT-qPCR Testing of SARS-CoV-2: A Primer. Int J Mol Sci. 2020;21(8):3004.
98. Ahrberg CD, Neužil P. Doubling Throughput of a Real-Time PCR. Sci Rep. 2015;5:12595.
99. Holland PM, Abramson RD, Watson R, Gelfand DH. Detection of specific polymerase chain reaction product by utilizing the 5'----3' exonuclease activity of Thermus aquaticus DNA polymerase. Proceedings of the National Academy of Sciences. 1991;88(16):7276-80.
100. van Diepen MT, Chapman R, Moore PL, Margolin E, Hermanus T, Morris L, et al. The adjuvant AlhydroGel elicits higher antibody titres than AddaVax when combined with HIV-1 subtype C gp140 from CAP256. PLOS ONE. 2018;13(12):e0208310.
101. Rodrigo AG, Goracke PC, Rowhanian K, Mullins JI. Quantitation of Target Molecules from Polymerase Chain Reaction-Based Limiting Dilution Assays. AIDS Research and Human Retroviruses. 1997;13(9):737-42.
102. Görzer I, Guelly C, Trajanoski S, Puchhammer-Stöckl E. The impact of PCR-generated recombination on diversity estimation of mixed viral populations by deep sequencing. Journal of Virological Methods. 2010;169(1):248-52.

103. Yang YL, Wang G, Dorman K, Kaplan AH. Long polymerase chain reaction amplification of heterogeneous HIV type 1 templates produces recombination at a relatively high frequency. AIDS Res Hum Retroviruses. 1996;12(4):303-6.
104. Meyerhans A, Vartanian JP, Wain-Hobson S. DNA recombination during PCR. Nucleic acids research. 1990;18(7):1687-91.
105. Kuo H-H, Lichterfeld M. Recent progress in understanding HIV reservoirs. Curr Opin HIV AIDS. 2018;13(2):137-42.
106. Chun TW, Moir S, Fauci AS. HIV reservoirs as obstacles and opportunities for an HIV cure. Nat Immunol. 2015;16(6):584-9.
107. Bailon L, Mothe B, Berman L, Brander C. Novel Approaches Towards a Functional Cure of HIV/AIDS. Drugs. 2020;80(9):859-68.
108. Deere JD, Kauffman RC, Cannavo E, Higgins J, Villalobos A, Adamson L, et al. Analysis of multiply spliced transcripts in lymphoid tissue reservoirs of rhesus macaques infected with RT-SHIV during HAART. PLoS One. 2014;9(2):e87914.
109. Siddiqui S, Perez S, Gao Y, Doyle-Meyers L, Foley BT, Li Q, et al. Persistent Viral Reservoirs in Lymphoid Tissues in SIV-Infected Rhesus Macaques of Chinese-Origin on Suppressive Antiretroviral Therapy. Viruses. 2019;11(2):105.
110. Bowles EJ, Schiffner T, Rosario M, Needham GA, Ramaswamy M, McGouran J, et al. Comparison of Neutralizing Antibody Responses Elicited from Highly Diverse Polyvalent Heterotrimeric HIV-1 gp140 Cocktail Immunogens versus a Monovalent Counterpart in Rhesus Macaques. PLOS ONE. 2014;9(12):e114709.